

# Transformations of Cyclic Olefins Mediated by Tungsten Nitrosyl Complexes

Miriam S. A. Buschhaus, Craig B. Pamplin, Ian J. Blackmore, and Peter Legzdins\*

Department of Chemistry, The University of British Columbia, Vancouver, British Columbia, Canada V6T 1Z1

Received May 1, 2008

This report describes investigations that have elucidated the nature, extent, and mechanism of the cyclic-olefin oligomerization effected by a series of tungsten precatalysts, with particular focus on  $\text{Cp}^*\text{W}(\text{NO})(\text{CH}_2\text{CMe}_3)_2$  (**1**) and  $\text{Cp}^*\text{W}(\text{NO})(\text{CH}_2\text{SiMe}_3)(\eta^2\text{-CPhCH}_2)$  (**2**). Upon thermolysis, these precatalysts oligomerize simple cyclic olefins, from cyclopentene to cyclooctene, into ring-retaining oligomers as high as dodecamers (depending on the substrate) with remaining sites of unsaturation. Precatalyst initiation involves the coupling of one equivalent of the substrate with the reactive 16e intermediate thermally generated by the precatalyst (i.e., an alkylidene by **1** or an  $\eta^2$ -alkyne complex by **2**), followed by rearrangement of the coupled ligand in the metal's coordination sphere either to an olefin or to a diene (with concomitant loss of two hydrogen atoms). The rearranged ligand is displaced from the metal center as two equivalents of substrate coordinate to form a putative bis-olefin complex,  $\text{Cp}^*\text{W}(\text{NO})(\text{cyclic olefin})_2$ , that represents the convergent entry point to the catalytic cycle for the precatalysts. The coordinated olefins undergo metal-mediated coupling to form a metallacyclopentane complex. The metallacycle then undergoes  $\beta$ -hydrogen activation and reductive elimination to generate an  $\eta^2$ -cyclic-olefin dimer. Further incorporation of substrate leads to formation of trimers and higher oligomers. Alternatively, expulsion of any coordinated oligomer from the tungsten center regenerates the reactive bis-olefin complex. Finally, decomposition of the tungsten catalyst species is consistent with a bimetallic pathway. All new organometallic complexes have been characterized by conventional spectroscopic and analytical methods, and the solid-state molecular structures of several compounds have been established by X-ray crystallographic analyses.

## Introduction

In recent years we have been investigating the characteristic chemistry of pseudo-octahedral  $\text{Cp}^*\text{M}(\text{NO})\text{R}_2$  complexes [ $\text{Cp}^* = \eta^5\text{-C}_5\text{Me}_5$ ; M = Mo or W; R = a hydrocarbyl group such as an alkyl, aryl, or allyl]. As part of these investigations, we have discovered that this family of complexes exhibits R-dependent thermal reactivity to form a variety of 16e nitrosyl complexes that are capable of effecting the single, double, or triple activation of hydrocarbon C–H bonds, often in a novel manner. These types of transformations are of considerable current interest, primarily due to the potential for eventual conversion of readily available hydrocarbons into more desirable products. One complex that we have studied extensively in this regard is the 16e tungsten nitrosyl complex,  $\text{Cp}^*\text{W}(\text{NO})(\text{CH}_2\text{CMe}_3)_2$  (**1**).<sup>1–3</sup> At 70 °C, complex **1** loses neopentane and forms the reactive alkylidene intermediate,  $\text{Cp}^*\text{W}(\text{NO})(=\text{CHCMe}_3)$  (**A**), which then initiates further chemistry. To date, our investigations of **1** have focused on the C–H bond activations initiated by the alkylidene intermediate **A** with aliphatic and aromatic

hydrocarbon substrates.<sup>1–3</sup> Most recently, we reported the ability of **A** to selectively activate the ortho C–H bonds of substituted benzenes.<sup>4</sup>

The present investigation extends our previous work and focuses on the reactivity of **1** with cyclic olefins. Preliminary experiments with these systems were conducted some years ago, and the results obtained then were not particularly encouraging. For example, it was found that thermolysis of **1** in cyclohexene is “accompanied by decomposition, formation of complex mixtures of organometallic side products, and the formation of organic byproducts, which unfortunately could not be quantified”.<sup>5</sup> Consequently, no further investigations with cyclic-olefin substrates were pursued at that time. In the interim, however, we have established that the congeneric molybdenum alkylidene complex  $\text{Cp}^*\text{Mo}(\text{NO})(=\text{CHCMe}_3)$  reacts with olefins and dienes to form molybdenacyclobutane complexes initially.<sup>6</sup> Interestingly, these complexes do not react further via olefin metathesis or cyclopropanation pathways, but rather via C–H activation. Armed with this knowledge, we have reexamined the tungsten alkylidene system and have discovered that while there are some similarities with the molybdenum congener, there also are some significant differences. The most striking difference that we have identified is that complex **1** and two other tungsten nitrosyl complexes, namely,  $\text{Cp}^*\text{W}(\text{NO})(\text{CH}_2\text{SiMe}_3)(\eta^2\text{-$

\* Corresponding author. E-mail: legzdins@chem.ubc.ca.

(1) Pamplin, C. B.; Legzdins, P. *Acc. Chem. Res.* **2003**, *36*, 223–233, and references therein.

(2) Legzdins, P.; Pamplin, C. B. Sequential Hydrocarbon C–H Bond Activations by 16-electron Organometallic Complexes of Molybdenum and Tungsten. In *Activation and Functionalization of C–H Bonds*; Goldberg, K. I., Goldman, A. S., Eds.; ACS Symposium Series 885; American Chemical Society: Washington, D.C., 2004; pp 184–197.

(3) Blackmore, I. J.; Jin, X.; Legzdins, P. *Organometallics* **2005**, *24*, 4088–4098, and references cited therein.

(4) Tsang, J. Y. K.; Buschhaus, M. S. A.; Legzdins, P.; Patrick, B. O. *Organometallics* **2006**, *25*, 4215–4225.

(5) Tran, E. Ph.D. Thesis, The University of British Columbia, Vancouver, Canada, 2001.

(6) (a) Graham, P. M.; Buschhaus, M. S. A.; Legzdins, P. *J. Am. Chem. Soc.* **2006**, *128*, 9038–9039. (b) Graham, P. M.; Buschhaus, M. S. A.; Pamplin, C. B.; Legzdins, P. *Organometallics* **2008**, *27*, 2840–2851.

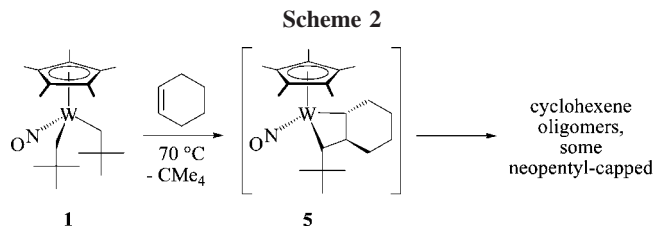
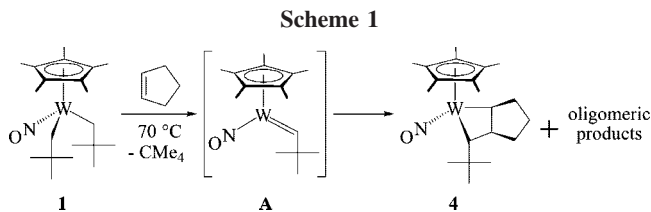


**Table 1. Comparison of the Characteristic  $^1\text{H}$  NMR Spectroscopic Resonances of the Molybdenum and Tungsten cis- and trans-Metallacycles**

Molybdenum	$^1\text{H}$ (ppm)	Tungsten	$^1\text{H}$ (ppm)
	H1: -0.05 (ddd) H2: 7.49 (dd) H6: 3.27 (d)		H1: -0.48 (m) H2: 7.65 (dt) H6: 3.18 (d)
	H1: -0.65 (m) H2: 0.1 (ddd) H7: 3.91 (d)		H1: -1.07 (m) H2: 0.09 (dq) H7: 3.64 (d)
	H1: -0.18 (ddd) H2: 4.10 (ddd) H9: 4.31 (d)		H1: -0.49 (dq) H2: 3.98 (dt) H9: 4.03 (d)

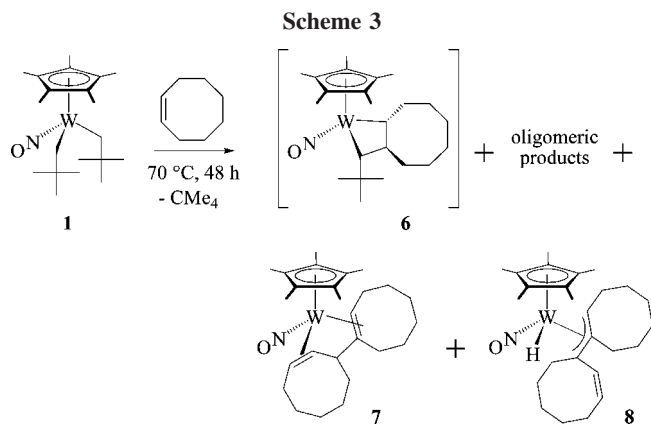
$\text{CPhCH}_2$ ) (**2**) and  $\text{Cp}^*\text{W}(\text{NO})[\text{CH}(\text{Ph})\text{CH}_2\text{CH}(\text{}^i\text{Pr})\text{CH}_2]$  (**3**), are precatalysts for the ring-retaining oligomerization of simple cyclic olefins, particularly cyclohexene. This article first describes the isolation and identification of both the organometallic products and the organic oligomers resulting from the reactions of **1** and **2** with cyclic olefins. It then examines the mechanisms by which these products are formed and proffers a united mechanistic rationale for precatalyst initiation and catalytic cyclic-olefin oligomerization.

## Results

**Reaction of 1 with Cyclopentene.** Thermolysis of **1** in cyclopentene at 70 °C yields orange complex **4** in 76% isolated yield and additional oligomeric products (Scheme 1).

To form **4**, the alkylidene intermediate **A** has simply undergone a 2 + 2 addition with cyclopentene to form the cis-metallacyclobutane. In the  $^1\text{H}$  NMR spectrum of **4** in  $\text{C}_6\text{D}_6$ , the three protons on the carbons of the metallacycle give rise to characteristic multiplets, specifically a downfield doublet of triplets centered at 7.65 ppm for the  $\alpha$ -hydrogen on the cyclopentane ring, a complex multiplet at -0.48 ppm for the  $\beta$ -hydrogen, and a doublet at 3.18 ppm for the  $\alpha$ -hydrogen nearest the  $^i\text{Bu}$  group. These spectral data are very similar to those exhibited by the analogous molybdenum cis-metallacycle,<sup>6</sup> as summarized for the various metallacyclobutane complexes in Table 1.

**Reaction of 1 with Cyclohexene.** The thermolysis products of **1** in cyclohexene include high yields of cyclohexene oligomers (*vide infra*) and an almost intractable mixture of organometallic compounds from which no individual species can be isolated. However, in the  $^1\text{H}$  NMR spectra of the crude product mixtures, one of the tungsten compounds gives rise to singlet methyl resonances at 1.74 ppm ( $\text{Cp}^*$ ) and 1.22 ppm ( $\text{CMe}_3$ ), to complex multiplets at -1.07 and 0.09 ppm, and to a doublet at 3.64 ppm. The splitting patterns of the three multiplet signals are similar to the characteristic resonances of



the previously characterized molybdenum trans-metallacycle of cyclohexene (Table 1).<sup>6</sup> The strong correlation in relative shift and splitting pattern in the  $^1\text{H}$  NMR spectra of the molybdenum and tungsten systems suggests that a tungsten trans-metallacycle (**5**) is among the products formed during the reaction of **1** with cyclohexene (Scheme 2). This conclusion confirms that the tungsten alkylidene intermediate can indeed react with the double bond of cyclohexene, presumably followed by further reaction and eventual decomposition of the initially formed metallacyclic complex.

**Reaction of 1 with Cyclooctene.** Thermolysis of **1** in cyclooctene at 70 °C for 48 h yields a mixture of products, which  $^1\text{H}$  NMR spectral analyses reveal to include at least three major organometallic compounds in addition to the organic products. The presence of a trans-metallacycle (**6**) is suggested by the  $^1\text{H}$  NMR spectroscopic data, but it cannot be isolated. The other two organometallic products can be separated from the mixture by chromatography on alumina in a combined yield of 38%. Fractional crystallization and solid-state X-ray crystallographic analyses reveal their respective molecular structures to be the 1,4-diene complex **7** and the allyl hydride **8** (Scheme 3).

The identity of compound **6** is deduced by comparison of its diagnostic  $^1\text{H}$  NMR spectroscopic peaks, as observed in the spectrum of the crude reaction mixture, with those of the analogous molybdenum compound.<sup>6</sup> Specifically, the three hydrogens of the metallacycle in **6** give rise to distinctive peaks at -0.49, 3.98, and 4.03 ppm, with splitting patterns of dq, dt, and d, respectively. The fully characterized molybdenum analogue gives rise to peaks with similar shift and splitting patterns (Table 1). Thus, like compound **5** above, compound **6** results from a coupling of the cyclic-olefin substrate with the alkylidene intermediate **A** to form a trans-metallacycle, and it provides another link between the observed tungsten and molybdenum products.

Compound **7** readily precipitates as a red solid from a cold  $\text{Et}_2\text{O}$  solution. Mass spectral analysis gives a parent mass of 567 amu, indicating the loss of the neopentyl ligands and the inclusion of two cyclooctene units at the metal center. The solid-state molecular structure confirms these changes and reveals the new ligand to be two coupled cyclooctene units connected to the metal center as a 1,4-diene (Figure 1). The solid-state

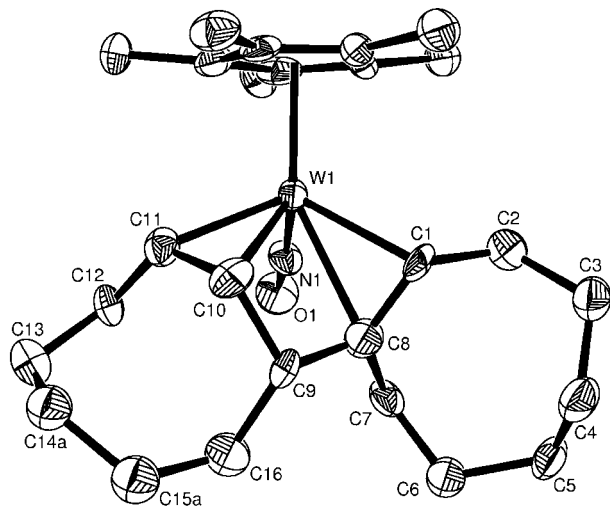


**Figure 1.** Solid-state molecular structure of **7** with 50% probability thermal ellipsoids. Selected interatomic distances (Å) and angles (deg): W(1)–C(1) = 2.283(10), W(1)–C(8) = 2.458(13), W(1)–C(10) = 2.264(13), W(1)–C(11) = 2.217(13), C(1)–C(8) = 1.390(17), C(8)–C(9) = 1.529(19), C(9)–C(10) = 1.505(16), C(10)–C(11) = 1.431(17), C(1)–C(8)–C(9) = 121.8(12), C(8)–C(9)–C(10) = 101.9(10), C(9)–C(10)–C(11) = 125.3(11), W(1)–N(1)–O(1) = 174.8(9).

molecular structure contains disorder at C14 and C15, which has been modeled as two parts contributing 70% and 30%, respectively. Nevertheless, the important structural details are unambiguous.

$^1\text{H}$  and  $^{13}\text{C}$  NMR spectroscopic analyses confirm that **7** retains its molecular structure in solution. Not surprisingly, the coupled cyclooctene ligand gives rise to many overlapping signals. The diagnostic peaks of the hydrogen and carbon atoms nearest the metal center can be readily assigned, but those of the  $\text{CH}_2$  groups are difficult to differentiate. The carbon signal of C1 appears at 72.1 ppm, and the related proton signal appears as a doublet of doublets at 2.14 ppm. The quaternary carbon C8 gives a peak at 69.4 ppm. The carbons of the other coordinated olefin give rise to peaks at 42.3 ppm (C10) and 47.5 ppm (C11). The olefinic proton signals appear as multiplets at 4.48 ppm (H10) and 0.90 ppm (H11). Finally, C9 gives rise to a peak at 9.5 ppm, and H9 to a triplet at  $-1.26$  ppm.

The other product isolated from the thermolysis of **1** in cyclooctene, namely **8**, recrystallizes as yellow prisms. Its parent mass is also 567 amu, and the solid-state molecular structure reveals that the coupled cyclooctene ligand is coordinated to the metal center through an allyl linkage (Figure 2). The metal center must also support a hydride ligand, as evidenced by the parent mass and the W–H signal observed by  $^1\text{H}$  NMR spectroscopy (*vide infra*). Unfortunately, the hydride could not be specifically located in the residual electron density map, despite the vacant coordination site on tungsten in the solid-state molecular structure. The coupled cyclooctene ligand contains an uncoordinated double bond between C10 and C11. Notwithstanding disorder in the  $\text{Cp}^*$  ligand, the final  $R$  value for the structure is 3.5%. The structures of **7** and **8** suggest that the complexes are formally related by way of a  $\beta$ -hydrogen C–H activation.

The NMR spectroscopic data for **8** again indicate that its solid-state molecular structure is retained in solution. In the  $^1\text{H}$  NMR spectrum the olefinic proton signals of H10 and H11 appear as a doublet at 7.00 ppm and a doublet of doublets of doublets at 5.17 ppm, respectively. The signal for the allyl proton

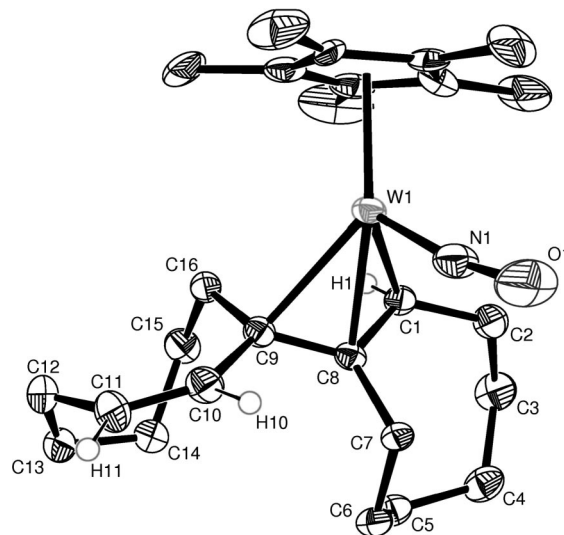


**Figure 2.** Solid-state molecular structure of **8** with 50% probability thermal ellipsoids. Selected interatomic distances (Å) and angles (deg): W(1)–C(1) = 2.279(3), W(1)–C(8) = 2.335(3), W(1)–C(9) = 2.472(3), C(1)–C(8) = 1.445(4), C(8)–C(9) = 1.422(4), C(9)–C(10) = 1.498(4), C(10)–C(11) = 1.353(5), C(1)–C(8)–C(9) = 118.0(3), C(8)–C(9)–C(10) = 118.0(3), C(9)–C(10)–C(11) = 130.9(3), W(1)–N(1)–O(1) = 169.7(3). The hydride ligand has not been located.

(H1) is buried under multiple methylene peaks at around 1.55 ppm. In the  $^{13}\text{C}$  NMR spectrum, the allylic carbons are indicated by peaks at 64.0 ppm (C1), 120.8 ppm (C8), and 91.2 ppm (C9). The carbon signals of the free olefin appear at 138.8 ppm (C10) and 119.1 ppm (C11). Signals due to the methylene groups of the coupled ligand are difficult to assign specifically. In the  $^{13}\text{C}$  NMR spectrum, 11 peaks appear between 20.9 and 35.0 ppm. In the  $^1\text{H}$  NMR spectrum, half of the methylene protons are represented by overlapping multiplets in the regions of 1.32 and 1.55 ppm. Signals for the methylene groups next to the allyl and olefin are spread over a greater range between 2.92 and 0.54 ppm. Finally, the hydride signal appears as a singlet at 0.12 ppm flanked by  $^{183}\text{W}$  satellites with a  $^1J_{\text{WH}}$  coupling constant of 124.6 Hz.

Monitoring the thermolysis of **7** in  $\text{C}_6\text{D}_6$  at 70 °C over 4 days by  $^1\text{H}$  NMR spectroscopy shows the decrease and almost complete loss of signals due to **7**. Peaks due to **8** appear and then eventually decrease with increasing time, thereby showing that **7** is able to convert to **8** under thermolysis conditions, followed by decomposition. Concomitant with the loss of **7** and **8** is the appearance of new multiplet peaks in the olefinic region, attributable to the release of the coupled cyclooctene molecule, presumably 1-cyclooct-3-enylcyclooctene. Regrettably, the splitting patterns of the peaks are not sufficiently resolved to be analyzed fully.

Thermolysis of **7** in cyclohexene at 70 °C for 24 h results in the formation of oligomers of cyclohexene, as identified by their characteristic signals at 1–2 and 5.3–5.8 ppm in the  $^1\text{H}$  NMR spectrum of the crude reaction mixture (Figure 3). Characteristic peaks for **7** and **8** also appear in an approximate 1:5 ratio, again confirming that **7** converts to **8** under thermolysis conditions in addition to forming the catalytically active species of the oligomerization cycle. Finally, strong singlets at 1.52 and 1.48 ppm suggest the formation of tungsten decomposition products.

**Reaction of 2 with Cyclohexene.** Other tungsten nitrosyl compounds that we have characterized previously, specifically precatalysts **2** and **3**, also oligomerize the cyclic olefins. We

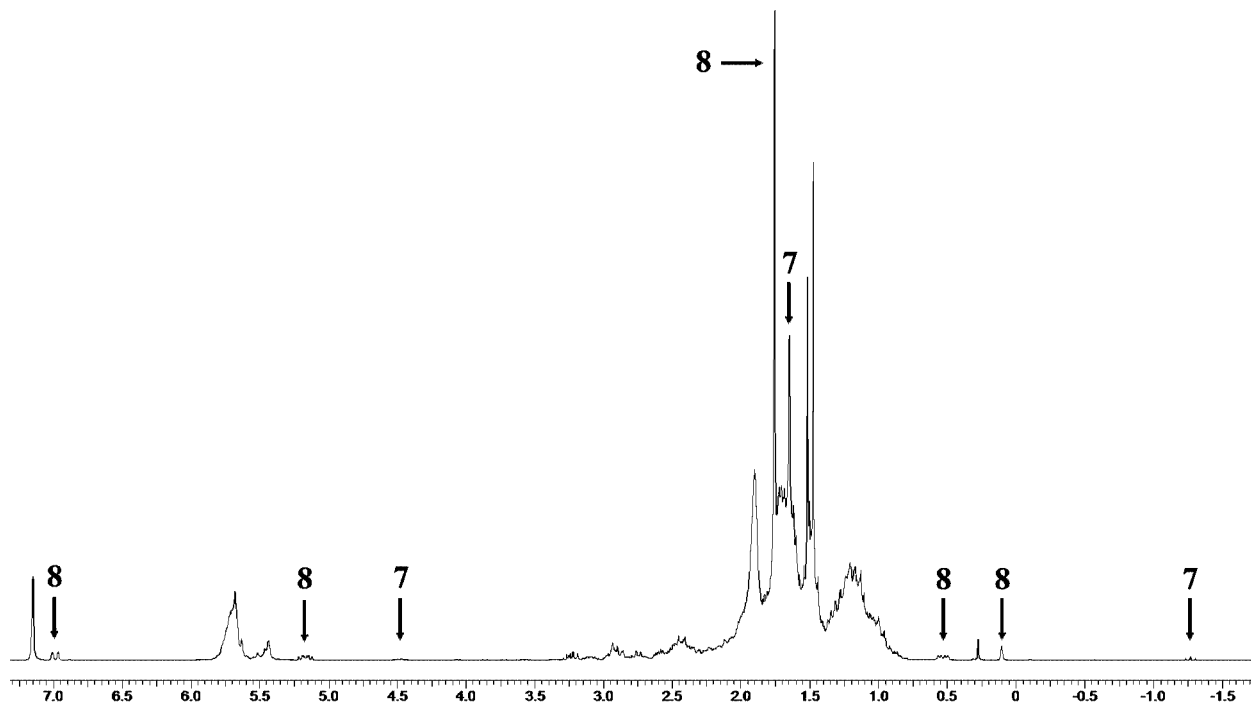
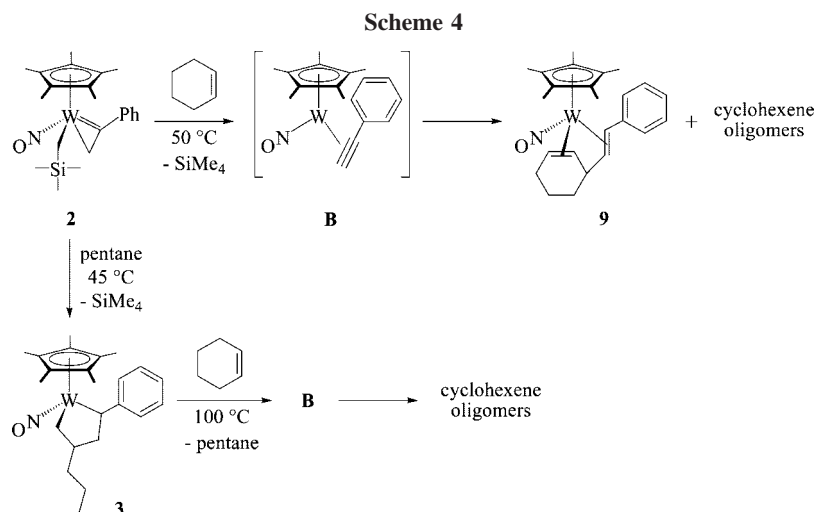


**Figure 3.**  $^1\text{H}$  NMR spectrum (300 MHz) of the product mixture from thermolysis of **7** in neat cyclohexene at 70 °C for 24 h, demonstrating the formation of cyclohexene oligomers, the formation of **8**, and the remaining presence of unreacted **7**. The arrows indicate diagnostic peaks due to **7** and **8**, while the cyclohexene oligomers give rise to broad peaks between 1–2 and 5.3–5.8 ppm.



focus here primarily on precatalyst **2** since **3** is derived from **2** by reaction with pentane<sup>7</sup> and reverts to the same reactive intermediate species (i.e., an  $\eta^2$ -alkyne complex, **B** in Scheme 4) with loss of pentane under thermolysis conditions. Consequently, **3** has been studied less extensively in oligomerization of cyclic olefins.

Thermolysis of **2** in cyclohexene at 50 °C for 24 h produces a dark red oil, the  $^1\text{H}$  NMR spectrum of which shows the presence of oligomers and one major organometallic species. Column chromatography of the oil on silica followed by recrystallization affords **9** in 27% yield (Scheme 4). The solid-state molecular structure of **9** is that of a 1,4-diene complex (Figure 4), and its characteristic spectroscopic properties confirm that it retains this molecular structure in solution.

To confirm that **9** is a precursor to the catalytic cycle and not merely a byproduct, an isolated sample has been dissolved

in cyclohexene and heated overnight at 50 °C. Analysis of the final product mixture by  $^1\text{H}$  NMR spectroscopy reveals the presence of cyclohexene oligomers and unreacted **9**, thereby indicating that it is indeed a precursor to the catalytically active species.

**The Oligomeric Products.** The organic products resulting from the reactions of **1** with various cyclic olefins (i.e., cyclohexene, 1,4-cyclohexadiene, cyclopentene, cyclooctene, and 4-methylcyclohexene) can be separated from the oily reaction residues by chromatography on alumina with pentane or hexanes as eluants to obtain clear, colorless, moderately viscous oils. Subsequent investigations have revealed that thermolysis of **1** in neat cyclic olefins at 100 °C for 24 h gives better turnover numbers than thermolysis at 70 °C for 40 h. Also, compounds **2** and **3** produce oligomers of similar composition and distribution when thermolyzed in the cyclic olefins at 100 °C for 24 h. Table 2 summarizes the variations

(7) Debad, J. D.; Legzdins, P.; Lumb, S.; Batchelor, R. J.; Einstein, F. W. B. *J. Am. Chem. Soc.* **1995**, *117*, 3288–3289.

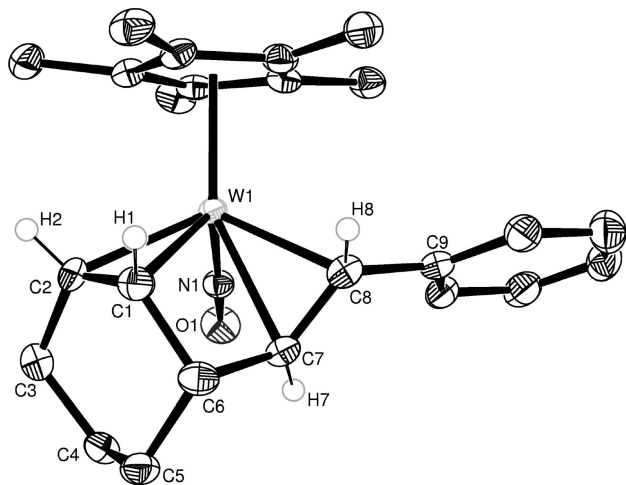


**Figure 4.** Solid-state molecular structure of **9** with 50% probability thermal ellipsoids shown. Selected interatomic distances (Å) and angles (deg): W(1)–C(1) = 2.269(4), W(1)–C(2) = 2.249(3), W(1)–C(7) = 2.388(4), W(1)–C(8) = 2.303(4), C(8)–C(7) = 1.392(6), C(7)–C(6) = 1.516(5), C(6)–C(1) = 1.517(5), C(1)–C(2) = 1.396(9), W(1)–N(1)–O(1) = 175.4(3), C(8)–C(7)–C(6) = 123.3(3), C(7)–C(6)–C(1) = 100.1(3), C(6)–C(1)–C(2) = 120.8(4).

**Table 2. Data for the Oligomerization of Cyclohexene**

precatalyst <sup>a</sup>	temperature (°C)	turnover number <sup>b</sup>	turnover frequency (h) <sup>b</sup>
<b>1</b>	70	69	1.7
<b>1</b>	100	148	6.2
<b>2</b>	100	131	5.5
<b>3</b>	100	157	6.5

<sup>a</sup> Precatalyst concentration 0.01 M. <sup>b</sup> Transfer hydrogenation processes (*vide infra*) were not taken into account when the number of molecules of cyclohexene oligomerized was calculated.

in precatalyst activity at concentrations of 0.01 M when cyclohexene is the substrate.

The isolated organic products are mixtures of ring-retaining oligomers, as characterized by <sup>1</sup>H NMR spectroscopy, low-resolution EIMS, and GC/MS. Small amounts of the oligomers are capped with a precatalyst-dependent end group (CH<sub>2</sub>CMe<sub>3</sub> or CH=CHPh). Our subsequent presentation of these results focuses on the more extensively characterized cyclohexene oligomers, while interesting insights and contrasts with the 1,4-cyclohexadiene oligomers are noted. Finally, characteristic features of the oligomers of cyclopentene, cyclooctene, and 4-methylcyclohexene are summarized briefly.

The cyclohexene oligomers retain unsaturated C=C linkages, as indicated by the presence of complex peaks in the region 5.4–5.8 ppm in their <sup>1</sup>H NMR spectra, in addition to larger signals at 1–2 ppm. Integration of the signals in the two regions gives an average aliphatic to olefinic proton ratio of 12:1. By contrast, a linear oligomer resulting from a ring-opening metathesis polymerization (ROMP) process would give a proton ratio of 4:1 regardless of chain length. Together with other evidence, particularly GC/MS analyses (*vide infra*), the experimental ratio suggests that the ring-motif of the cyclohexene substrate is retained in the oligomers.

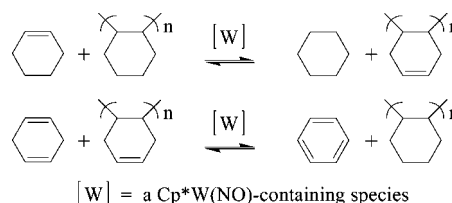
The low-resolution EIMS of the cyclohexene oligomer mixture displays groups of peaks separated by 80 to 82 amu. The largest peak in each group is tabulated in Table 3 and is compared to the degree of oligomerization and to the predicted mass for a monounsaturated ring-retaining cyclohexene oligomer. It is evident that as the oligomer length increases, the degree of unsaturation increases as well. The highest oligomer

**Table 3. Mass Spectral Data for Cyclohexene and 1,4-Cyclohexadiene Oligomers**

<i>n</i>	cyclohexene oligomers		1,4-cyclohexadiene oligomers	
	predicted mass	observed mass <sup>a</sup>	predicted mass	observed mass <sup>b</sup>
2	164	163	160	160 (161)
3	246	243	240	241 (244)
4	328	325	320	321 (324)
5	410	405	400	402 (409)
6	492	487	480	483 (487)
7	574	568	560	563 (568)
8	656	650	640	643 (649)
9	738	730	720	724 (728)
10	820	812	800	803 (N/A)

<sup>a</sup> Largest peak in the envelope listed. <sup>b</sup> Largest peak in the envelope listed with the highest *m/z* peak listed in parentheses.

**Scheme 5**



mass detected for a cyclohexene oligomer corresponds to a decamer having five C=C unsaturations.

Interestingly, a EIMS analysis of the 1,4-cyclohexadiene oligomers shows similar degrees of oligomerization, a decamer being the largest species detected. This time, however, the oligomers have gained mass compared to predicted values (Table 3). Thus, the second highest mass detected for a 1,4-cyclohexadiene oligomer corresponds to a nonamer with at least four fewer C=C linkages than expected.

The varying levels of unsaturation in the cyclohexene and 1,4-cyclohexadiene oligomers tabulated in Table 3 can be attributed to a transfer dehydrogenation process. When the *in situ* reaction mixture derived from the thermolysis of **2** in cyclohexene at 60 °C for 24 h is examined by <sup>1</sup>H NMR spectroscopy, a peak due to cyclohexane appears at 1.83 ppm in the spectrum, and higher than predicted levels of unsaturation appear in the cyclohexene oligomers (*vide supra*). Conversely, similar analysis of the reaction mixture of **2** in 1,4-cyclohexadiene shows the appearance of a peak at 7.16 ppm due to the formation of benzene and a small peak at 1.37 ppm due to cyclohexane, while the 1,4-cyclohexadiene oligomers contain lower levels of unsaturation than predicted. Scheme 5 illustrates the net results of the transfer dehydrogenation process. In the case of the 1,4-cyclohexadiene oligomerization, the formation of benzene likely provides the driving force for the transfer of hydrogen from 1,4-cyclohexadiene to the oligomers. The driving force for the reverse transfer dehydrogenation reaction when cyclohexene is the substrate is not as clear.

Analysis by GC/MS gives further information about the composition of the cyclohexene oligomer mixture. A typical GC trace of the cyclohexene oligomers derived from precatalyst **1** has clusters of peaks (Figure 5), and each cluster can be identified with discrete oligomer lengths, namely, cyclohexene dimers, trimers, tetramers, and pentamers. Oligomers higher than pentamers are difficult to detect, as they represent only a small fraction of the total oligomer volume. In addition, small peaks due to dimers and trimers capped with a neopentyl group are present at 6.2 min and at about 12 min, respectively.

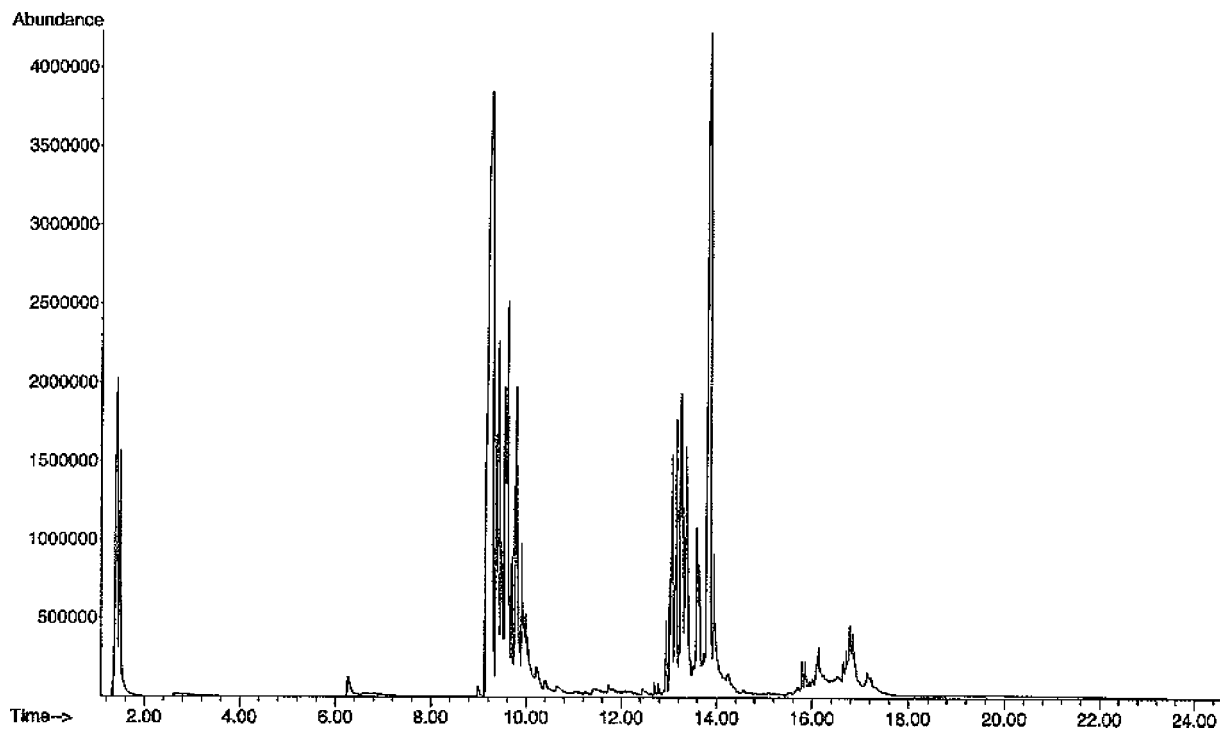


Figure 5. Typical GC trace for the mixture of cyclohexene oligomers (min, standard method).

Table 4. Summary of GC and MS Data for the Cyclohexene Oligomers Produced by 1

oligomer group	no. of peaks	elution times (min)	parent masses detected	empirical formulas	no. of unsaturations
dimers	2–3	1.4–1.6	166, 164, 162	C <sub>12</sub> H <sub>22,20,18</sub>	0, 1, 2
dimer + npt <sup>a</sup>	1	6.2–6.4	234	C <sub>17</sub> H <sub>30</sub>	1
trimers	11–16	9–10	246, 244	C <sub>18</sub> H <sub>30,28</sub>	1, 2
tetramers	15–16	13–14	326, 324	C <sub>24</sub> H <sub>38,36</sub>	2, 3
pentamers	4–12 <sup>b</sup>	15.5–17.5	408, 406	C <sub>30</sub> H <sub>48,46</sub>	2, 3
higher	3–12 <sup>b</sup>	19–24	488+ <sup>c</sup>	C <sub>36</sub> H <sub>56</sub>	3 or more

<sup>a</sup> npt = neopentyl. <sup>b</sup> The number of peaks visible above the baseline noise varies greatly from sample to sample. <sup>c</sup> The MS detects from 0 to 500 amu, so the exact parent masses beyond 488 are unknown.

Each peak within a cluster represents a unique compound. Thus, the more than 11 peaks in the trimer cluster (Figure 1,  $t = 9–11$  min) correspond to more than 11 trimeric oligomers differing in ring connectivity and in unsaturation levels. The variable unsaturation levels are demonstrated in each peak's associated mass spectrum. Thus, for the cyclohexene dimer cluster, three distinct parent masses of 166, 164, and 162 are identified that correspond to zero, one, and two unsaturations per dimer. Similarly, in the trimer cluster each peak's parent mass corresponds to either one or two unsaturations being present in each unique trimer. These data are presented in Table 4.

The relative percentages of each type of cyclohexene oligomer present in the mixture are obtained by integration of the GC peaks. Typical values from the best analyses indicate a distribution of 7% dimers, 45% trimers, 36% tetramers, 10% pentamers, and 1% higher oligomers. The integrated percentages for each oligomer length are not affected by choice of precatalyst. However, the neopentyl-capped oligomers from precatalyst **1** under thermolysis conditions of 70 °C comprise about 1% of the mixture, as determined from the GC trace.

In the mass spectra associated with each peak in the GC trace, the individual cyclohexene oligomers fragment in a distinctive pattern that indicates the sequential loss of six-carbon units with variable unsaturation levels of zero and one C=C bond in each unit. The fragmentation patterns confirm that the ring structure of the monomer is retained in the oligomer. If the substrate had

been oligomerized by a ring-opening process, the expected fragmentation pattern would be that of a linear unsaturated hydrocarbon, namely, loss of C<sub>n</sub>H<sub>2n</sub> units with a relatively large representation of two-carbon and three-carbon units.<sup>8</sup> In addition, a cyclohexene dimer capped with a neopentyl group fragments in a manner consistent with retention of the ring structure, losing either a cyclohexyl or a neopentyl group.

Various methods have been employed during attempts to separate the cyclohexene oligomer mixture into its component parts, whether by oligomer length or by individual compounds. Selective dissolutions using different solvent mixtures, HPLC, and TLC do not give the desired results. Vacuum distillation of the cyclohexene oligomer mixture gives reasonable separation of the lowest oligomer families. At 10<sup>-3</sup> mm Hg, two fractions distill at 55 and 116–120 °C, respectively. According to GC/MS analyses, the first fraction contains 100% cyclohexene dimers, and the second fraction contains up to 94% trimers, with some dimer and tetramer contamination. The oligomers that remain undistilled are a combination of trimers (20%), tetramers (56%), and higher oligomers (24%).

The isolated cyclohexene dimers have been further characterized by NMR spectroscopic analyses. The experimental aliphatic to olefinic proton ratio of 7:1 suggests an average of between one and two unsaturations per dimer over the entire dimer

(8) Pavia, D. L.; Lampman, G. M.; Kriz, G. S. *Introduction to Spectroscopy*, 2nd ed.; Saunders College Publishing: Orlando, 1996.

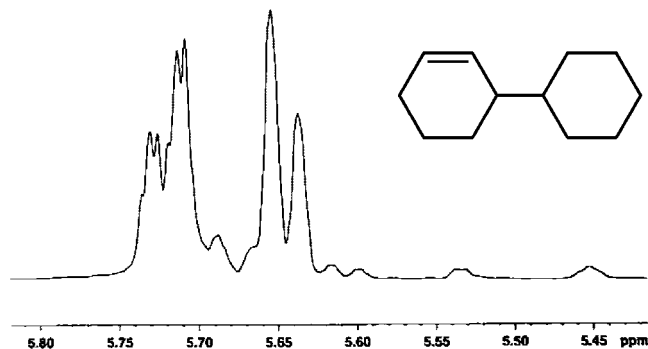


**Figure 6.** Expansion showing the characteristic olefinic peaks of 3-cyclohexylcyclohexene in the  $^1\text{H}$  NMR spectrum (600 MHz,  $\text{C}_6\text{D}_6$ ).

mixture. This is in agreement with GC/MS data, which indicate small amounts of a dimer with no unsaturations and larger amounts of dimers with one and two unsaturations. The  $^{13}\text{C}$  NMR spectrum for the cyclohexene dimer mixture shows at least 13 olefinic carbon peaks in the region between 127 and 132 ppm, reflecting the variety of isomers as well as the differing unsaturation levels.

Hydrogenation of the cyclohexene dimer mixture yields the fully saturated dimer cyclohexylcyclohexane as the only product. Complete NMR spectroscopic analyses confirm the identification and support the ring-retaining structure of the oligomer. A second, incomplete hydrogenation reaction affords two products in a 1:2 ratio. The first is identified as cyclohexylcyclohexane. The second is an unsaturated cyclohexene dimer, identified as 3-cyclohexylcyclohexene on the basis of its  $^1\text{H}$  and  $^{13}\text{C}$  NMR spectroscopic data. Specifically, the  $^1\text{H}$  NMR spectrum displays two complex resonances between 5.63 and 5.74 ppm, each of which integrates for one hydrogen, and the total integration suggests that the dimer is monounsaturated. The splitting patterns of the olefinic multiplets are complicated by the AB pairing of the peaks, but roughly resemble a broad doublet and a doublet of doublets (Figure 6). The  $^{13}\text{C}$  NMR spectrum displays two olefinic peaks at 127.4 and 131.2 ppm, and the entirety of the  $^1\text{H}$  and  $^{13}\text{C}$  NMR spectra can be consistently assigned to 3-cyclohexylcyclohexene. Comparison of the key resonances of 3-cyclohexylcyclohexene to those appearing in the NMR spectra of the original cyclohexene dimer mixture reveals that this compound is the major isomer of the monounsaturated cyclohexene dimers.

**Other Substrates.** Precatalyst **1** oligomerizes cyclic olefins to varying extents (Table 5). The organic products formed from cyclopentene conform to the general characteristics previously described for the cyclohexene oligomers. Cyclopentene oligomer lengths consistently range from dimers to undecamers or dodecamers ( $m/z = 810$ ), and unsaturation levels increase with oligomer length, with up to four double bonds in the longest oligomers. In the complex GC trace, peaks for dimers through septamers can be identified; however, integration is unreliable due to overlapping peaks. The yield of cyclopentene oligomer per mole of **1** is lower than that of cyclohexene. Calculated according to the entire amount of **1**, a turnover number of 5.6 is obtained. However, taking into account the amount of unreacted cis-metallacycle **4** (*vide supra*) recovered, the turnover number is 24 moles of cyclopentene per mole of active tungsten catalyst.

The cyclooctene oligomers also exhibit similar characteristics, with ring-retaining structure and a predominance of shorter oligomers. Integration of the  $^1\text{H}$  NMR spectroscopic resonances

indicates an aliphatic to olefinic proton ratio of 9:1, suggesting an average of between one to two unsaturations per two cyclooctene units. Mass spectroscopic analyses detect peaks for dimers and trimers with two unsaturations, and for higher oligomers from tetramers to septamers with one unsaturation. A GC/MS analysis indicates that neopentyl groups are coupled to both cyclooctene and cyclooctene dimers (with one or two unsaturations) and that multiple isomers of cyclooctene dimers and trimers with two unsaturations are present. The calculated turnover number is 1.45, based on the total amount of **1**. The relatively small conversion ratio suggests that the large ring size slows the rate of reaction, a feature that is also observed for the analogous molybdenum system.<sup>6</sup>

The products of 4-methylcyclohexene with **1** as the precatalyst are complex. The organometallic products cannot be isolated, and oligomer yield is low.

Precatalyst **2** oligomerizes cyclopentene, cyclohexene, and 1,4-cyclohexadiene to yield ring-retaining products analogous to those described above for **1**. In the EIMS of the 1,4-cyclohexadiene products, peaks are detected corresponding to oligomers capped with a vinyl end group,  $\text{CH}=\text{CHPh}$ , in addition to the peaks representing oligomers derived only from the substrate. However, 1,3-cyclohexadiene does not oligomerize under thermolysis conditions. This negative result with 1,3-cyclohexadiene indicates that 1,4-cyclohexadiene is not isomerized during its oligomerization.<sup>9</sup>

**Concentration Dependence of Precatalyst 1.** The activity of precatalyst **1** in cyclohexene is concentration dependent, with greater substrate turnover being achieved at lower concentrations. Figure 7 illustrates the general trend for representative samples of **1** thermolyzed in cyclohexene for 40 h at 70 °C. Concentrations of 0.005–0.010 M give optimal conversions.

## Discussion

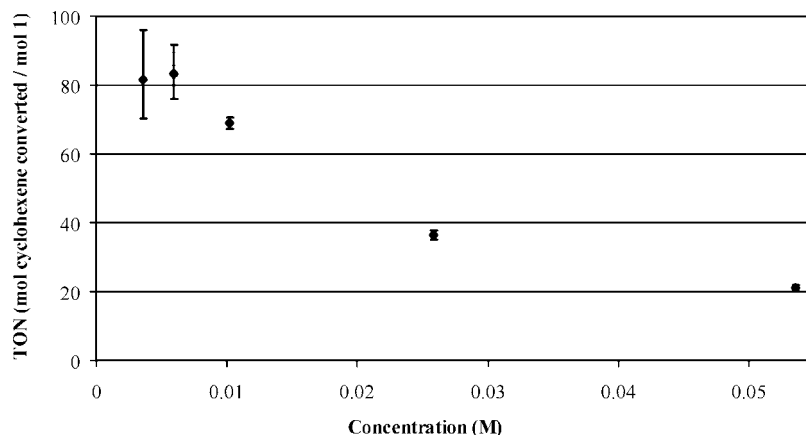
**Initiation Pathways.** The initiation pathway of precatalyst **1** has been elucidated by comparison to its molybdenum analogue,  $\text{Cp}^*\text{Mo}(\text{NO})(\text{CH}_2\text{CMe}_3)_2$ .<sup>6</sup> As shown in Scheme 6, both compounds generate reactive alkylidene intermediates of the form  $[\text{Cp}^*\text{M}(\text{NO})(=\text{CHCMe}_3)]$  ( $\text{M} = \text{W}$  or  $\text{Mo}$ ) via intramolecular  $\alpha$ -hydrogen abstraction. The alkylidene intermediates then react with the substrate cyclic olefin via a 2 + 2 addition to form a metallacyclobutane. In both systems, the cis-metallacycle derived from cyclopentene can be isolated, and the cis-metallacycles derived from larger ring sizes isomerize to trans-metallacycles. During the thermolysis of **1**, the tungsten trans-metallacycles derived from cyclohexene and cyclooctene (**5**, **6**) can be detected by  $^1\text{H}$  NMR spectroscopy, but signals due to the putative preceding cis-metallacycles have not been observed. The molybdenum trans-metallacycles convert to  $\eta^4$ -diene complexes with concomitant loss of dihydrogen, and under thermolysis conditions the coupled organic ligand can dissociate from the metal center and allow a small amount of cyclic-olefin oligomerization, particularly of cyclohexene.<sup>6</sup> Additionally, the reported catalytic dimerization of allylbenzene necessitates the loss of a coupled organic containing the neopentyl group.<sup>6</sup> In contrast, the tungsten trans-metallacycles do not persist at the temperatures required to generate the alkylidene intermediate

(9) In contrast, many systems (based on radical, anionic, cationic, transition-metal, or rare-earth-metal catalysts) are known to polymerize 1,3-cyclohexadiene. For some recent examples, see. (a) Li, X.; Baldamus, J.; Nishiura, M.; Tardif, O.; Hou, Z. *Angew. Chem., Int. Ed.* **2006**, *45*, 8184–8188, and references therein. (b) Longo, P.; Freda, C.; Ruiz de Ballesteros, O.; Grisi, F. *Macromol. Chem. Phys.* **2001**, *202*, 409–412, and references therein.

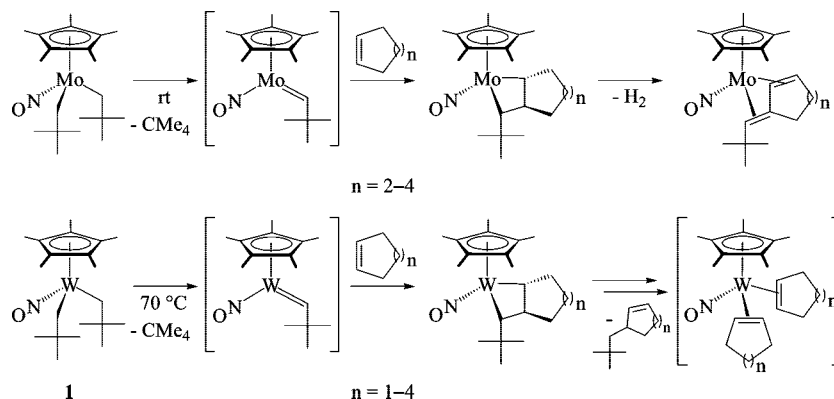
**Table 5.** Comparison of the Cyclic-Olefin Substrates Oligomerized by Precatalyst **1** Based on Turnover Number (TON) and Oligomer Distribution

substrate	TON <sup>a</sup>	oligomer distribution (percentage by GC) <sup>b</sup>						
		olefin + npt	dimer	dimer + npt	trimer	trimer + npt	tetramer	pentamer and higher
cyclohexene	83, <sup>c</sup> 149 <sup>d</sup>		7	1	45		36	11
1,4-cyclohexadiene	163 <sup>d</sup>		12		32		38	18
cyclopentene	24 <sup>e</sup>				not assigned			
cyclooctene	1.45	6	90	2	1			
4-methylcyclohexene	0.4			9	72	3	16	

<sup>a</sup> TON = mol substrate converted per mol **1**. <sup>b</sup> Olefin = cyclic-olefin substrate, npt = neopentyl. <sup>c</sup> Best result at 70 °C. <sup>d</sup> At 100 °C. <sup>e</sup> Calcd based on active catalyst formed.



**Figure 7.** Effect of variable initial concentrations of **1** in cyclohexene on catalyst activity (turnover number, after 70 °C, 40 h). Error bars are calculated on the basis of uncertainties of  $\pm 2$  mg of **1** and  $\pm 10$  mg of oligomer recovered.

**Scheme 6**

**A**, and the coupled ligand converts to a coordinated olefin by  $\beta$ -hydrogen transfer. Subsequent loss of the olefin and coordination of 2 equiv of the cyclic substrate then form the proposed catalytic species  $\text{Cp}^*\text{W}(\text{NO})(\text{cyclic olefin})_2$ . Thus, as summarized in Scheme 6, the initiation of precatalyst **1** follows a reaction pathway analogous to that established for the molybdenum analogue, but then readily proceeds into the catalytic oligomerization of the cyclic olefins.

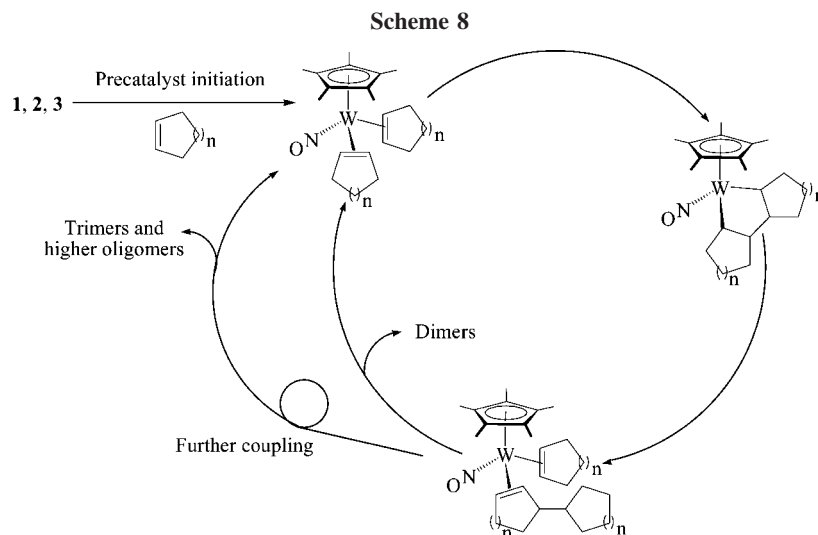
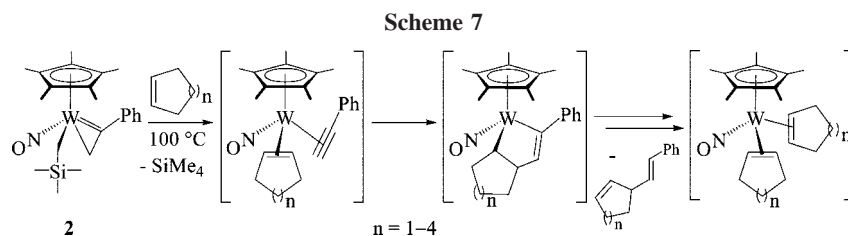
The initiation of precatalyst **2** begins with formation of the reactive  $[\text{Cp}^*\text{W}(\text{NO})(\eta^2\text{-HC}\equiv\text{CPh})]$  (**B**), the intermediate  $\eta^2$ -alkyne complex known to be formed by gentle thermolysis of **2**.<sup>7,10</sup> Complex **B** coordinates a molecule of the cyclic olefin, and the two ligands then couple to form a metallacycle, which subsequently converts via the activation and transfer of a  $\beta$ -hydrogen to a 1,4-diene complex, an example of which (**9**)

has been isolated (Scheme 7). Finally, loss of the 1,4-diene ligand and coordination of 2 equiv of the cyclic substrate form the putative  $\text{Cp}^*\text{W}(\text{NO})(\text{cyclic olefin})_2$  complex. Precatalyst **3** undergoes similar reactions after initial formation of **B** with loss of pentane.

As outlined above, the cyclohexene oligomers produced by precatalysts **2** and **3** are identical in form and distribution to those produced by precatalyst **1**, with the exception of the small percentage of oligomers having capping end groups. These end groups (i.e.,  $\text{CH}=\text{CHPh}$  or  $\text{CH}_2\text{CMe}_3$ ) vary with the precatalyst employed and reflect the initiation steps of the catalytic mechanism. This commonality in the products from different starting complexes suggests that variable initiation routes lead to a common catalytic cycle. However, it is highly unlikely that the  $14e$   $[\text{Cp}^*\text{W}(\text{NO})]$  fragment exists unligated by substrate in solution. Therefore, the solvated  $\text{Cp}^*\text{W}(\text{NO})(\text{cyclic olefin})_2$  complex, as shown in Schemes 6 and 7, is proposed as a reasonable representation of the  $[\text{Cp}^*\text{W}(\text{NO})]$ -containing species.

(10) Debad, J. D.; Legzdins, P.; Lumb, S. A.; Rettig, S. J.; Batchelor, R. J.; Einstein, F. W. B. *Organometallics* **1999**, *18*, 3414, and references therein.





**The Catalytic Cycle.** The proposed  $\text{Cp}^*\text{W}(\text{NO})(\text{cyclic olefin})_2$  complex represents the entry point into the catalytic cycle after precatalyst initiation, as illustrated in Scheme 8. The cyclic olefins couple in the tungsten's coordination sphere to form a metallacyclopentane, a structural motif for which literature precedents exist.<sup>11,12</sup> Subsequent  $\beta$ -hydrogen activation and transfer yields a dihapto cyclic-olefin dimer, which may then either couple to a third molecule of the substrate or be displaced to regenerate the initial bis-olefin complex. In this way, ring-retaining oligomers of various lengths and configurations are obtained. While none of the species in the catalytic cycle have been directly observed, the coupling of the cyclic olefins in the coordination sphere of the tungsten complex is further substantiated by the isolation of the 1,4-diene complex **7** and the allyl hydride complex **8**, in which two molecules of cyclooctene have been coupled together.

Four  $\beta$ -hydrogens are available to the metal center in the simple metallacyclopentane complex illustrated in Scheme 8, and due to the symmetry of the tungstenacycle, two possible dimer products could result. Consistent with the mechanism presented, the major monounsaturated cyclohexene dimer in the oligomer mixture is 3-cyclohexylcyclohexene. For any unsymmetrical metallacycle, such as occurs during the formation of trimers and higher oligomers, up to four different isomers can form upon elimination. Theoretically, 12 unique trimers are predicted by the proposed mechanism, which correlates with the experimentally observed cluster of many trimer peaks observed in GC/MS analyses of the cyclohexene oligomers. The further complexity of the isolated cyclohexene oligomers (multiple unsaturations) is accounted for by the previously

established transfer dehydrogenation process. The detection of cyclohexene oligomers capped with neopentyl or  $\text{CH}=\text{CPh}$  end groups indicates that the coupled olefins formed during initiation via precatalysts **1** and **2** participate in the coupling reactions in the catalytic cycle.

The proposed catalytic cycle is also consistent with the formation of compounds **7** and **8** during the thermolysis of **1** in cyclooctene. As illustrated in Scheme 9, the formation of the metallacyclopentane is followed by activation of a  $\beta$ -hydrogen. Subsequent transfer of H to the ligand creates a monounsaturated cyclooctene dimer that may be released from the metal center. In contrast, a loss of two hydrogen atoms forms a ligand with two unsaturations, as exists in **7**. From that point a reversible  $\beta$ -hydrogen elimination forms the allyl hydride **8**, or dissociation of the ligand produces the experimentally observed dimers having two unsaturations and regenerates the tungsten bis-cyclic-olefin catalyst.

**Catalyst Decomposition.** The active tungsten oligomerization catalyst probably decomposes via a bimetallic reaction pathway. The observed inverse trend between solution concentrations and turnover numbers (Figure 7) indicates that another reaction (or perhaps several) is occurring that diverts the catalyst out of the catalytic cycle and that this reaction is discouraged at lower concentrations. The decomposition product(s) of the tungsten nitrosyl precatalysts have not been identified. In this connection it may be noted that the tungsten and molybdenum alkylidene metathesis catalysts of Schrock also exhibit bimolecular decomposition pathways.<sup>13</sup> Both the experimental evidence and comparisons to related systems in the literature support the plausibility of a bimetallic decomposition pathway for the reactive  $\text{Cp}^*\text{W}(\text{NO})(\text{cyclic olefin})_2$  species and its derivatives.

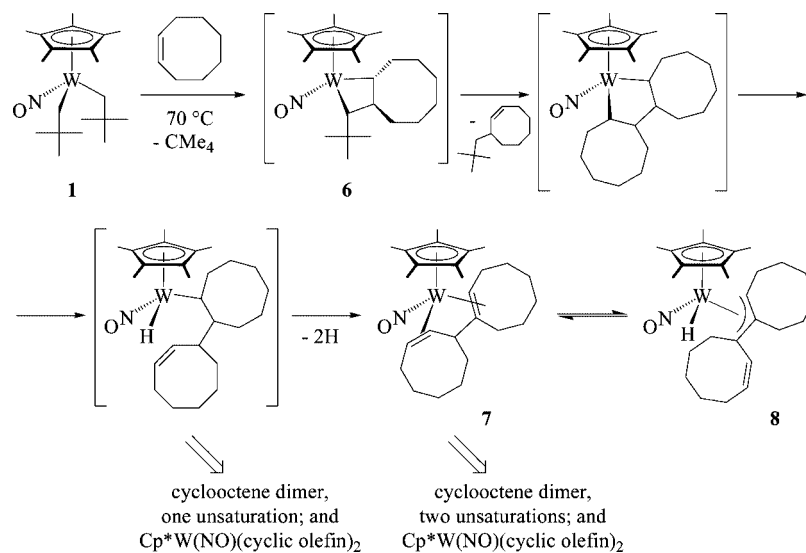
**Mechanistic Explanations for Other Cyclic-Olefin Couplings Mediated by  $\text{Cp}^*\text{M}(\text{NO})$  Compounds.** The coupling mechanism proposed in Scheme 8 to explain the oligo-

(11) For proposals of intermediate metallacyclopentanes, see: (a) McLain, S. J.; Schrock, R. R. *J. Am. Chem. Soc.* **1978**, *100*, 1315–1317. (b) You, Y.; Wilson, S. R.; Girolami, G. S. *Organometallics* **1994**, *13*, 4655–4657.

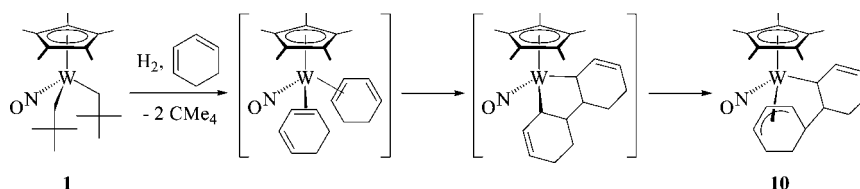
(12) For examples of isolable metallacyclopentanes, see: (a) Ison, E. A.; Abboud, K. A.; Boncella, J. M. *Organometallics* **2006**, *25*, 1557–1564. (b) Arndt, S.; Schrock, R. R.; Müller, P. *Organometallics* **2007**, *26*, 1279–1290.

(13) Schrock, R. R.; Czekelius, C. *Adv. Synth. Catal.* **2007**, *349*, 55–77, and references therein.

Scheme 9



Scheme 10



merization of simple cyclic olefins by precatalysts **1** and **2** can also be extended to rationalize the formation of other coupled products that we have previously observed.

Thus, hydrogenolysis of **1** under 1 atm of dihydrogen at 20 °C in the presence of cyclohexene or 1,3-cyclohexadiene forms alkyl-allyl complexes.<sup>14</sup> The neopentyl ligands are converted to neopentane, and a bis-olefin tungsten adduct forms, as illustrated in Scheme 10 for the 1,3-cyclohexadiene-derived product **10**. Subsequent coupling to form a metallacycle, followed by coordination of a double bond beside one of the alkyl links to form an  $\eta^3$ -allyl, accounts for the observed product and lends strong support to the proposed metallacyclopentane complex. An X-ray crystallographic analysis of **10** reveals both the  $\eta^3, \eta^1$ -binding motif of the organic ligand and the additional uncoordinated double bond (Figure 8). In the related case with cyclohexene, a loss of two hydrogen atoms is necessary to form the observed alkyl-allyl product.

We have also previously reported a second system that couples two molecules of a cyclic-olefin substrate under hydrogenolysis conditions.<sup>15</sup> In this case, a general method had been developed to react  $\text{Cp}^*\text{M}(\text{NO})(\text{CH}_2\text{SiMe}_3)_2$  ( $\text{M} = \text{Mo}$  or  $\text{W}$ ) with  $\text{H}_2$  and acyclic dienes at low temperatures to lose 2 equiv of tetramethylsilane and generate  $\eta^4$ -trans-diene complexes. However, when 1,3-cyclooctadiene was employed as the diene, the resulting product (**11**) had two molecules of the substrate coupled in the metal's coordination sphere. A single-crystal X-ray crystallographic analysis of **11** established that the organic ligand was 2-cyclooct-2-en-1-yl-1,3-cyclooctadiene, a triene coordinated to the metal center in a bis- $\eta^2$  fashion. While no mechanistic insight was proffered at the time that these results

were communicated,<sup>15</sup> application of the ideas of an initial bis-olefin complex followed by coupling in the metal's coordination sphere to form a metallacycle,  $\beta$ -hydrogen activation and rearrangement can readily rationalize this reactivity, as shown in Scheme 11.

**Comparisons to Earlier Systems and to Alkylidene Metathesis Catalysts.** In general, when cyclic olefins are used as substrates in metathesis reactions the result is ring-opening

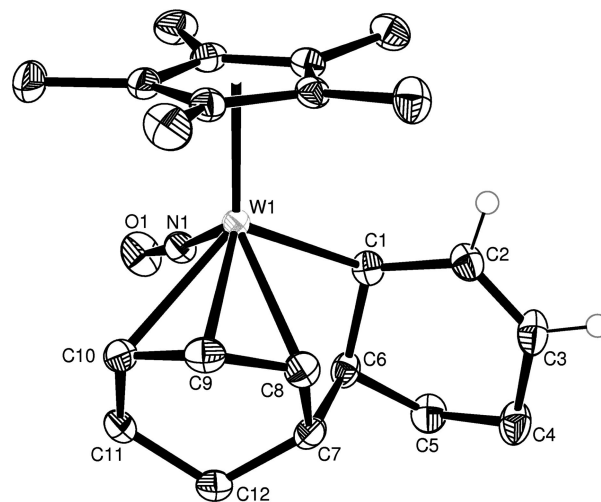
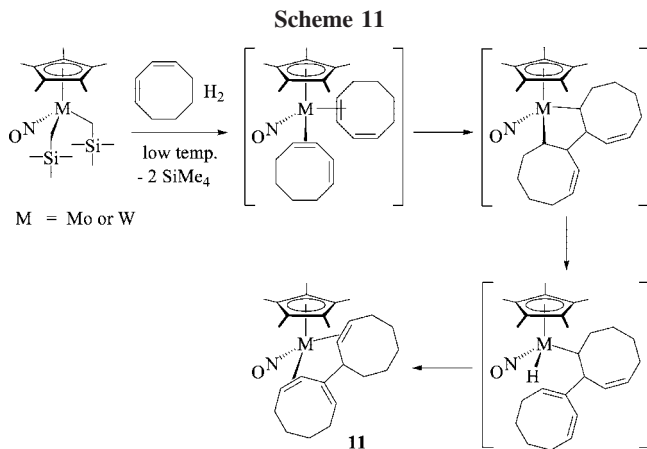


**Figure 8.** Solid-state molecular structure of **10** with 50% probability thermal ellipsoids. Selected interatomic distances (Å) and angles (deg):  $\text{W}(1)-\text{C}(1) = 2.272(2)$ ,  $\text{W}(1)-\text{C}(8) = 2.295(2)$ ,  $\text{W}(1)-\text{C}(9) = 2.283(2)$ ,  $\text{W}(1)-\text{C}(10) = 2.424(2)$ ,  $\text{C}(1)-\text{C}(2) = 1.502(3)$ ,  $\text{C}(2)-\text{C}(3) = 1.334(3)$ ,  $\text{C}(1)-\text{C}(6) = 1.558(3)$ ,  $\text{C}(6)-\text{C}(7) = 1.566(3)$ ,  $\text{C}(7)-\text{C}(8) = 1.531(3)$ ,  $\text{C}(8)-\text{C}(9) = 1.417(3)$ ,  $\text{C}(9)-\text{C}(10) = 1.399(3)$ ,  $\text{W}(1)-\text{C}(1)-\text{C}(6) = 103.66(13)$ ,  $\text{C}(1)-\text{C}(2)-\text{C}(3) = 125.0(2)$ ,  $\text{C}(1)-\text{C}(6)-\text{C}(7) = 109.11(16)$ ,  $\text{C}(6)-\text{C}(7)-\text{C}(8) = 109.86(18)$ ,  $\text{C}(7)-\text{C}(8)-\text{C}(9) = 120.5(2)$ ,  $\text{C}(8)-\text{C}(9)-\text{C}(10) = 118.9(2)$ ,  $\text{W}(1)-\text{N}(1)-\text{O}(1) = 173.66(17)$ .

(14) For the cyclohexene-derived product, see: Jin, X.; Legzdins, P.; Buschhaus, M. S. A. *J. Am. Chem. Soc.* **2005**, *127*, 6928–6929, and unpublished observations.

(15) Debad, J. D.; Legzdins, P.; Young, M. A.; Batchelor, R. J.; Einstein, F. W. B. *J. Am. Chem. Soc.* **1993**, *115*, 2051–2052.



to generate linear oligomers or polymers by ROMP.<sup>16,17</sup> However, the cyclic olefin must have sufficient ring strain to react in this manner.<sup>17</sup> Thus, ring-opening metathesis polymerization of norbornene, cyclopentene, cyclooctene, and their derivatives is common, while similar processes for cyclohexene are almost unknown.<sup>18</sup>

Two early olefin-metathesis experiments conducted in 1975 and 1980 report the ring-retaining oligomerization of cyclohexene. These experiments, based on  $WCl_6$  in conjunction with a variety of additives to form ill-defined, yet catalytically active, reaction mixtures, produce oligomers similar to those obtained with precatalysts **1** and **2**, but with much lower levels of unsaturation.<sup>19,20</sup> The original reports provide very little mechanistic insight, but later work has demonstrated that olefin metathesis is not the mechanism. One report suggests the involvement of a tungsten hydride species that forms an adduct with cyclohexene and subsequently reacts.<sup>20</sup>

In contrast, the oligomerization reactions described here begin with discrete precatalyst complexes whose initiation pathways can be determined, and the proposed catalytic cycle is supported by a variety of observations including several isolated organometallic complexes containing two substrate molecules coupled in the metal's coordination sphere. The proposed mechanisms do not contain any species with both a hydride and a coordinated cyclic olefin. The transient hydride species proposed to form during the coupling of the cyclic olefins contain either an alkyl or an allyl linkage to the organic ligand, and an allyl hydride (**8**) has been isolated. Thus, hydride species analogous to those proposed in 1980 are neither invoked nor observed in the present system.

It is of interest that **1**, which forms a reactive alkylidene intermediate upon thermolysis, produces oligomers of cyclic olefins such as cyclopentene and cyclooctene but shows no signs of ROMP activity. The crucial involvement of alkylidene complexes in olefin metathesis has been known for many years and is amply demonstrated in the metathesis catalysts of Schrock

and Grubbs.<sup>16,17,21,22</sup> Comparisons between our group-6 alkylidene complexes and those of Schrock reveal several key differences that ultimately result in very different modes of reactivity. The Schrock alkylidenes can be isolated and fully characterized, and during metathesis reactions some of the alkylidene complexes propagating the polymerization can be observed by NMR spectroscopy. Metallacyclobutane complexes are proposed as intermediate species, but they are generally not detectable.<sup>21</sup> In contrast, our alkylidenes derived from **1** and  $Cp^*Mo(NO)(CH_2CMe_3)_2$  under thermolysis conditions are undetectable, highly reactive intermediates,<sup>1</sup> and the metallacycles resulting from coupling with cyclic olefins are the isolable or spectroscopically detectable species (*vide supra*). Both our and the Schrock alkylidene complexes are electron deficient; however, the Schrock metathesis catalysts are formally  $d^0$ , while our nitrosyl precatalysts are formally  $d^4$ . Thus, our complexes are relatively electron rich at the metal center, in large part because the nitrosyl ligand stabilizes the  $d^4$  metal. It is these differences that we believe result in our alkylidene complexes possessing their unique reactivity.

## Conclusion

These investigations have elucidated the nature, extent, and mechanism of the cyclic-olefin oligomerization reactivity observed with a series of tungsten precatalysts, with particular focus on  $Cp^*W(NO)(CH_2CMe_3)_2$  (**1**) and  $Cp^*W(NO)(CH_2SiMe_3)(\eta^2-CPhCH_2)$  (**2**). Under thermolysis conditions these tungsten precatalysts initiate oligomerization of simple cyclic olefins, from cyclopentene to cyclooctene, into ring-retaining oligomers as high as dodecamers (depending on the substrate) with remaining sites of unsaturation. The mechanistic rationale provides a unified explanation for the observed precatalyst initiation reactions and the catalytic cyclic-olefin oligomerization. Precatalyst initiation involves the coupling of 1 equiv of the substrate with the reactive  $16e$  intermediate typically generated by the precatalyst (i.e., an alkylidene or an  $\eta^2$ -alkyne complex), followed by rearrangement of the coupled ligand to an olefin or to a diene with loss of two hydrogen atoms. The coupled ligand is displaced from the metal center as 2 equiv of substrate coordinate to form a bis-olefin complex,  $Cp^*W(NO)(cyclic\ olefin)_2$ , that represents the convergent entry point to the catalytic cycle for the precatalysts. The coordinated olefins undergo metal-mediated coupling to form a metallacyclopentane complex. The metallacycle then undergoes  $\beta$ -hydrogen activation and reductive elimination to generate a cyclic-olefin dimer as a coordinated olefin. Further addition and coupling of substrate leads to formation of trimers and higher oligomers. Alternatively, loss of the coordinated oligomer regenerates the reactive bis-olefin complex. Finally, decomposition of the tungsten catalyst species is consistent with a bimetallic pathway.

The investigations described provide unique insights in two major areas: (1) the mechanism for formation of ring-retaining oligomers from cyclic olefins, with particular focus on cyclohexene and the tungsten nitrosyl precatalysts **1** and **2**, and (2) the reactivity of the alkylidene intermediate formed from **1** (i.e., **A**) with cyclic olefins in a manner distinct from the ROMP reactivity commonly observed for other tungsten and molybdenum alkylidene systems.

(16) Ivin, K. J.; Mol, J. C. *Olefin Metathesis and Metathesis Polymerization*; Academic Press: San Diego, 1997, and references therein.

(17) *Handbook of Metathesis*; Grubbs, R. H., Ed.; Wiley-VCH: Weinheim, 2003; Vols. 1–3: *Catalyst Development* (Vol. 1); *Applications in Organic Synthesis* (Vol. 2); *Applications in Polymer Synthesis* (Vol. 3), and references therein.

(18) Small amounts of ROMP-derived cyclohexene oligomers can be observed in metathesis reactions carried out at very low temperatures; see: Patton, P. A.; Lillya, C. P.; McCarthy, T. J. *Macromolecules* **1986**, *19*, 1266–1268.

(19) Mouljijn, J. A.; van de Noulant, B. M. *React. Kinet. Catal. Lett.* **1975**, *3*, 405–408.

(20) Giezynski, R.; Korda, A. *J. Mol. Catal.* **1980**, *7*, 349–354.

(21) (a) Schrock, R. R.; Czekelius, C. *Adv. Synth. Catal.* **2007**, *349*, 55–77, and references therein. (b) Schrock, R. R. *J. Mol. Catal. A: Chem.* **2004**, *213*, 21–30, and references therein.

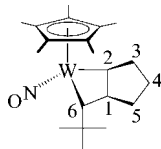
(22) Grubbs, R. H. *Tetrahedron* **2004**, *60*, 7117–7140, and references therein.

## Experimental Section

**General Methods.** All reactions and subsequent manipulations involving organometallic reagents were performed under anaerobic and anhydrous conditions either at a vacuum-nitrogen dual manifold or in an inert-atmosphere drybox. Pentane, benzene-*d*<sub>6</sub>, diethyl ether, hexanes, and tetrahydrofuran (THF) were all dried over sodium benzophenone ketyl and were freshly distilled prior to use. Cyclopentene, cyclohexene, cyclooctene, 1,4-cyclohexadiene, 1,3-cyclohexadiene, and 4-methylcyclohexene were all purchased from Aldrich and were dried over sodium benzophenone ketyl, distilled, and stored in resealable glass vessels. Cp\*W(NO)(CH<sub>2</sub>CMe<sub>3</sub>)<sub>2</sub> (**1**),<sup>23</sup> Cp\*W(NO)(CH<sub>2</sub>SiMe<sub>3</sub>)(η<sup>2</sup>-CPhCH<sub>2</sub>) (**2**),<sup>10</sup> and Cp\*W(NO)[CH(Ph)CH<sub>2</sub>-CH(<sup>n</sup>Pr)CH<sub>2</sub>] (**3**)<sup>10</sup> were prepared according to the published procedures. All other chemicals were purchased from Aldrich and were used as received.

All IR samples were prepared as Nujol mulls sandwiched between NaCl plates, and their spectra were recorded on a Thermo Nicolet model 4700 FT-IR spectrometer. NMR spectra were recorded at room temperature on Bruker AV-300, Bruker AV-400, Bruker AV-500, or Bruker AV-600 instruments, and all chemical shifts and coupling constants are reported in ppm and in hertz, respectively. <sup>1</sup>H NMR spectra were referenced to the residual protio isotopomer present in C<sub>6</sub>D<sub>6</sub> (7.15 ppm). <sup>13</sup>C NMR spectra were referenced to C<sub>6</sub>D<sub>6</sub> (128 ppm). Where necessary, <sup>1</sup>H-<sup>1</sup>H COSY, <sup>1</sup>H-<sup>13</sup>C HMQC, <sup>1</sup>H-<sup>13</sup>C HMQC, and <sup>13</sup>C APT experiments were carried out to correlate and assign <sup>1</sup>H and <sup>13</sup>C NMR signals. GC/MS analyses were carried out on an Agilent 6890 Series GC system equipped with a nonpolar, cross-linked 5% diphenyl-, 95% dimethylpolysiloxane column and an Agilent 5973 Network mass-selective detector. High- and low-resolution mass spectra (EI, 70 eV) were recorded by the staff of the UBC mass spectrometry facility using a Kratos MS-50 spectrometer. Elemental analyses were performed by Mr. Minaz Lakha of the UBC microanalytical facility.

**Reaction of 1 with Cyclopentene: Preparation of 4.** A red 0.02 M solution of **1** (0.050 g, 0.102 mmol) in cyclopentene (5.0 mL) was maintained at 70 °C for 49.5 h, and the final reaction mixture was orange-red. The volatiles were removed *in vacuo*. The reaction residue was redissolved in Et<sub>2</sub>O and placed in a -32 °C freezer overnight. An orange precipitate was isolated and identified as the metallacycle **4** (0.038 g, 0.078 mmol, 76% yield). The remaining reaction products were chromatographed on an alumina column (3 × 0.5 cm) with pentane and Et<sub>2</sub>O as eluents. A colorless oil (0.039 g) was recovered from the pentane eluate, and a bronze-brown residue (0.018 g) was recovered from the Et<sub>2</sub>O eluate.



Anal. Calcd for C<sub>20</sub>H<sub>33</sub>WNO: C, 49.29; H, 6.83; N, 2.87. Found: C, 49.59; H, 7.03; N, 2.89. <sup>1</sup>H NMR (C<sub>6</sub>D<sub>6</sub>, 300 MHz, 25 °C): δ -0.48 (1H, m, *H*<sub>1</sub>), 0.16 (1H, m, *H*<sub>5</sub>), 1.17 (9H, s, CMe<sub>3</sub>), 1.53 (1H, m, CH<sub>2</sub>), 1.74 (15H, s, C<sub>5</sub>Me<sub>5</sub>), 2.07 (1H, m, CH<sub>2</sub>), 2.21 (1H, m, CH<sub>2</sub>), 2.45 (1H, m, *H*<sub>3</sub>), 3.18 (1H, d, <sup>3</sup>*J*<sub>HH</sub> = 4.9, *H*<sub>6</sub>), 7.65 (1H, dt, <sup>3</sup>*J*<sub>HH</sub> = 8.2, <sup>3</sup>*J*<sub>HH</sub> = 11.4, *H*<sub>2</sub>). One CH<sub>2</sub> proton signal is obscured, presumably under one of the strong methyl singlets. <sup>13</sup>C{<sup>1</sup>H} NMR (C<sub>6</sub>D<sub>6</sub>, 125 MHz, 25 °C): δ 10.2 (C<sub>5</sub>Me<sub>5</sub>), 15.9 (C<sub>1</sub>), 32.5 (CMe<sub>3</sub>), 33.7 (C<sub>3</sub>, C<sub>4</sub> or C<sub>5</sub>), 37.6 (C<sub>3</sub>, C<sub>4</sub> or C<sub>5</sub>), 40.3 (C<sub>3</sub>, C<sub>4</sub> or C<sub>5</sub>), 41.6 (CMe<sub>3</sub>), 108.9 (C<sub>5</sub>Me<sub>5</sub>), 115.0 (C<sub>6</sub>), 139.9 (C<sub>2</sub>). MS (EI, 120 °C): *m/z* 487 [P<sup>+</sup>].

(23) Debad, J. D.; Legzdins, P.; Rettig, S. J.; Veltheer, J. E. *Organometallics* **1993**, *12*, 2714–2725.

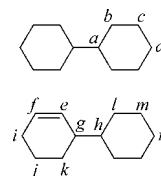
Isolated oligomeric products MS (EI, 150 °C → 300 °C): *m/z* 135, 201, 269, 337, 405, 473, 540, 608, 676, 744 [P<sup>+</sup>].

**Oligomerization of Cyclohexene Effected by 1.** The thermolysis of **1** in cyclohexene was carried out at various concentrations, reaction times, and reaction temperatures. A representative reaction is described here. A red 0.05 M solution of **1** (0.108 g, 0.220 mmol) in cyclohexene (4.1 mL) was thermolyzed at 70 °C for 40 h to obtain a dark brown solution. The volatiles were removed *in vacuo*, and the reaction residue was a dark brown oil that flowed easily (0.501 g). The residue was completely dissolved in pentane and chromatographed on an alumina column (5 × 0.5 cm). The pentane eluate (ca. 10 mL) yielded a clear oil (0.379 g). Et<sub>2</sub>O and THF eluates were also collected, and they afforded dark brown residues (0.061 and 0.021 g, respectively) after solvent removal.

**Characterization of the Oligomeric Products.** The oligomers were characterized by EIMS (320 °C) and <sup>1</sup>H NMR spectroscopy. GC/MS samples were prepared by dissolving a few drops of the oligomers in Et<sub>2</sub>O. A standard method was employed with an initial column temperature of 120 °C for 5 min, followed by a temperature ramp of 15 °C/min over 12 min up to 300 °C, and a final hold at 300 °C for 15 min.

**Vacuum Distillation of the Cyclohexene Oligomer Mixture.** The distillation of the cyclohexene oligomer mixture (5.3 g) was set up with a silicone oil bath and a Vigreux distillation column packed with glass beads. The system was placed under dynamic vacuum, and the mixture was heated with stirring. A first fraction (1.9 g) distilled at 55 °C, and a second fraction (1.0 g) distilled at 116–120 °C. The oil remaining in the still pot constituted a third fraction. The viscosity of the still pot contents was noticeably greater than that of the distilled fractions, and that of the second fraction greater than the first fraction. A small amount of each fraction was dissolved in Et<sub>2</sub>O and analyzed by GC/MS utilizing a method analogous to that employed for the oligomer mixture.

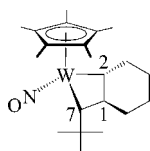
**Hydrogenation of the Cyclohexene Dimers.** A sample of previously distilled cyclohexene dimers (0.435 g, ~0.5 mL) was injected into a flask containing Wilkinson's catalyst (0.045 g) dissolved in benzene (15 mL) under a hydrogen atmosphere. After being vigorously stirred overnight, the reaction was stopped, the solvent was removed *in vacuo*, and the residue was redissolved in pentane and filtered through a Florisil column (3 × 1 cm). The organic products were collected and analyzed by NMR spectroscopy. The major product was identified as cyclohexylcyclohexane. A second reaction (0.91 g of distilled cyclohexene dimers, 0.103 g of Wilkinson's catalyst, 20 mL of benzene) was performed in a similar manner for 3 h. The hydrogenation of the dimers was not yet complete, and two major products were present, identified as cyclohexylcyclohexane and 3-cyclohexylcyclohexene.



**Characterization Data for the Mixture of Cyclohexylcyclohexane and 3-Cyclohexylcyclohexene.** <sup>1</sup>H NMR (600 MHz, C<sub>6</sub>D<sub>6</sub>, 25 °C): δ 0.9–1.06 (2H, *b*; 2H, *l*; 1H, *a*), 1.08–1.24 (1H, *d*; 1H, *n*; 1H, *h*; 2H, *c*; 2H, *m*), 1.27–1.34 (1H, *k*), 1.44–1.51 (1H, *j*), 1.57–1.77 (1H, *k'*; 1H, *d'*; 1H, *n'*; 1H, *b'*; 1H, *l'*; 1H, *j'*; 2H, *c'*; 2H, *m'*), 1.88–1.94 (1H, *g*; 2H, *i*), 5.63–5.67 (1H, *e*), 5.70–5.74 (1H, *f*). All signals were complex, overlapping multiplets whose *J* values could not be determined. <sup>13</sup>C{<sup>1</sup>H} NMR (150 MHz, C<sub>6</sub>D<sub>6</sub>, 25 °C): δ 22.7 (*j*), 25.8 (*i*), 26.1 (*k*), 27.1, 27.2 (three peaks; *m*, *m'*, *n*), 27.3 (*c* and *d*), 30.1 (*l* or *l'*), 30.5 (*b*), 30.6 (*l* or *l'*), 41.3 (*g*), 43.0 (*h*), 43.8 (*a*), 127.4 (*f*), 131.2 (*e*).

**Identification of 5.** Key resonances of compound **5** were identified by <sup>1</sup>H NMR spectroscopy of the crude reaction residue

resulting from the thermolysis of **1** in cyclohexene and of the mixture of organometallic products obtained by chromatography on alumina with pentane and Et<sub>2</sub>O as eluants. Complex **5** could not be isolated in a pure state.

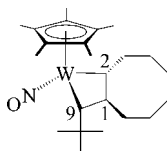


Selected resonances for **5** obtained from a 7:1 pentane/Et<sub>2</sub>O fraction: <sup>1</sup>H NMR (C<sub>6</sub>D<sub>6</sub>, 500 MHz, 25 °C): δ -1.07 (1H, m, *H1*), 0.09 (1H, dq, <sup>3</sup>J<sub>HH</sub> = 4.8, <sup>3</sup>J<sub>HH</sub> = 13.1, *H2*), 1.22 (9H, s, *CMe<sub>3</sub>*), 1.74 (15H, s, *C<sub>5</sub>Me<sub>5</sub>*), 3.64 (1H, d, <sup>3</sup>J<sub>HH</sub> = 4.6, *H7*).

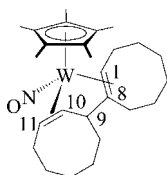
**Reaction of 1 with 4-Methylcyclohexene.** A red 0.16 M solution of **1** (0.1006 g, 0.205 mmol) in 4-methylcyclohexene (1.3 mL) was treated in a manner analogous to the cyclohexene reactions described above to obtain oligomeric products (8 mg), which were subjected to GC/MS and an intractable mixture of organometallic products (71 mg).

**Reaction of 1 with 1,4-Cyclohexadiene.** A red 0.011 M solution of **1** (0.040 g, 0.081 mmol) in 1,4-cyclohexadiene (7.1 mL) was thermolyzed at 100 °C for 24 h and worked up in a manner analogous to the cyclohexene reactions described above to obtain a crude product mixture of dark oil (1.261 g). Part of this mixture (0.315 g) was chromatographed on alumina with pentane to obtain oligomeric products as a clear, colorless oil (0.267 g), which was then subjected to GC/MS.

**Reaction of 1 with Cyclooctene: Identification of 6 and Preparation of 7 and 8.** A red 0.01 M solution of **1** (0.203 g, 0.413 mmol) in cyclooctene (41.0 mL) was thermolyzed at 70 °C for 48 h. The volatiles were removed *in vacuo*, and the reaction residue (0.321 g) was analyzed by <sup>1</sup>H NMR spectroscopy. Complex **6** was identified on the basis of characteristic NMR signals in the spectra. The reaction residue was then chromatographed on an alumina column (3.5 × 2 cm) with pentane and Et<sub>2</sub>O as eluants. A clear, slightly yellowish oil (0.066 g) was recovered from the pentane eluate, and an orange-red residue (0.090 g) was recovered from the Et<sub>2</sub>O eluate. The orange-red residue was selectively extracted with pentane to obtain a red solid (0.056 g, 0.099 mmol, 24%) and an orange solution. The red solid was dissolved in THF, and pentane was diffused into the solution at room temperature to induce the formation of small red crystals of **7**. Yellow crystals of **8** deposited together with red crystals of **7** from the orange solution upon cooling, and they were separated by hand.

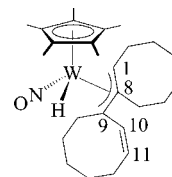


Compound **6**: selected <sup>1</sup>H NMR resonances (C<sub>6</sub>D<sub>6</sub>, 300 MHz, 25 °C): δ -0.49 (1H, dq, <sup>3</sup>J<sub>HH</sub> = 11.6, <sup>3</sup>J<sub>HH</sub> = 3.4, *H1*), 1.69 (15H, s, *C<sub>5</sub>Me<sub>5</sub>*), 3.98 (1H, dt, <sup>3</sup>J<sub>HH</sub> = 10.0, <sup>3</sup>J<sub>HH</sub> = 4.5, *H2*), 4.03 (1H, d, <sup>3</sup>J<sub>HH</sub> = 4.2, *H9*).



Compound **7**: IR (Nujol): ν<sub>NO</sub> 1577 (s) cm<sup>-1</sup>. <sup>1</sup>H NMR (C<sub>6</sub>D<sub>6</sub>, 400 MHz, 25 °C): δ -1.26 (1H, pseudo t, <sup>3</sup>J<sub>HH</sub> = 10.2, *H9*),

0.90 (1H, ddd, <sup>3</sup>J<sub>HH</sub> = 6.3, <sup>3</sup>J<sub>HH</sub> = 9.9, <sup>3</sup>J<sub>HH</sub> = 11.3, *H11*), 1.19 (1H, m, CH<sub>2</sub>), 1.38 (4H, m, CH<sub>2</sub>), 1.58 (3H, m (obscured), CH<sub>2</sub>), 1.65 (15H, s, *C<sub>5</sub>Me<sub>5</sub>*), 1.71 (3H, m (obscured), CH<sub>2</sub>), 1.84 (3H, m, CH<sub>2</sub>), 1.92 (3H, m, CH<sub>2</sub>), 2.14 (1H, dd, <sup>3</sup>J<sub>HH</sub> = 2.8, <sup>3</sup>J<sub>HH</sub> = 10.5, *H1*), 2.30 (3H, m, CH<sub>2</sub>), 2.45 (2H, m, CH<sub>2</sub>), 4.48 (1H, m, *H10*). <sup>13</sup>C{<sup>1</sup>H} NMR (C<sub>6</sub>D<sub>6</sub>, 100 MHz, 25 °C): δ 9.5 (C9), 10.1 (C<sub>5</sub>Me<sub>5</sub>), 26.6 (CH<sub>2</sub>), 26.7 (CH<sub>2</sub>), 27.5 (CH<sub>2</sub>), 27.8 (CH<sub>2</sub>), 28.2 (CH<sub>2</sub>), 28.9 (CH<sub>2</sub>), 30.7 (CH<sub>2</sub>), 31.7 (CH<sub>2</sub>), 31.9 (CH<sub>2</sub>), 32.7 (CH<sub>2</sub>), 34.6 (CH<sub>2</sub>), 42.3 (C10), 47.5 (C11), 69.4 (C8), 72.1 (C1), 102.1 (C<sub>5</sub>Me<sub>5</sub>). HRMS-EI *m/z*: [M<sup>+</sup>] calcd for <sup>184</sup>WNOC<sub>26</sub>H<sub>41</sub> 567.26977; found 567.26968.



Compound **8**: IR (Nujol): ν<sub>NO</sub> 1589 (s) cm<sup>-1</sup>. <sup>1</sup>H NMR (C<sub>6</sub>D<sub>6</sub>, 400 MHz, 25 °C): δ 0.12 (1H, s with satellites, <sup>1</sup>J<sub>WH</sub> = 124.6, *WH*), 0.54 (1H, dd, <sup>2</sup>J<sub>HH</sub> = 14.7, <sup>3</sup>J<sub>HH</sub> = 6.7, CH<sub>2</sub>), 1.32 (7H, overlapping m, CH<sub>2</sub>), 1.55 (5H, overlapping m, *H1* and CH<sub>2</sub>), 1.76 (15H, s, *C<sub>5</sub>Me<sub>5</sub>*), 1.93 (3H, overlapping m, CH<sub>2</sub>), 2.03 (1H, m, CH<sub>2</sub>), 2.22 (1H, m, CH<sub>2</sub>), 2.44 (2H, overlapping m, CH<sub>2</sub>), 2.92 (3H, overlapping m, CH<sub>2</sub>), 5.17 (1H, ddd, <sup>3</sup>J<sub>HH</sub> = 12.4, <sup>3</sup>J<sub>HH</sub> = 9.6, <sup>3</sup>J<sub>HH</sub> = 7.3, *H11*), 7.00 (1H, d, <sup>3</sup>J<sub>HH</sub> = 12.4, *H10*). <sup>13</sup>C{<sup>1</sup>H} NMR (C<sub>6</sub>D<sub>6</sub>, 100 MHz, 25 °C): δ 10.4 (C<sub>5</sub>Me<sub>5</sub>), 20.9 (CH<sub>2</sub>), 26.0 (CH<sub>2</sub>), 26.7 (CH<sub>2</sub>), 27.5 (CH<sub>2</sub>), 28.4 (CH<sub>2</sub>), 28.7 (CH<sub>2</sub>), 29.7 (CH<sub>2</sub>), 31.0 (CH<sub>2</sub>), 31.7 (CH<sub>2</sub>), 32.1 (CH<sub>2</sub>), 35.0 (CH<sub>2</sub>), 64.0 (C1), 91.2 (C9), 105.3 (C<sub>5</sub>Me<sub>5</sub>), 119.1 (C11), 120.8 (C8), 138.8 (C10). MS (EI, 100 °C): *m/z* 567 [P<sup>+</sup>].

**Isolated Oligomeric Products.** <sup>1</sup>H NMR (C<sub>6</sub>D<sub>6</sub>, 400 MHz, 25 °C): δ 0.85–0.95, 1.2–1.75, 1.90–2.50, 3.10–3.25, 5.2–5.4, 5.4–5.55, 5.6–5.8; aliphatic to olefinic proton ratio 9:1. MS (EI, 150 °C → 300 °C): *m/z* 218, 328. MS (EI, 150 °C): *m/z* 441, 551, 661, 771.

**<sup>1</sup>H NMR Spectra of 7 in C<sub>6</sub>D<sub>6</sub> and in Cyclohexene after Heating.** A sample of **7** dissolved in C<sub>6</sub>D<sub>6</sub> was thermolyzed at 70 °C for 4 days and monitored daily by <sup>1</sup>H NMR spectroscopy. Resonances due to **7** decreased over the reaction time. Resonances due to **8** appeared and increased over the first 48 h and then decreased again. Multiplet peaks due to organic products appeared in the ranges 1–2.5 and 5.3–5.8 ppm. Many singlet peaks attributed to decomposition products appeared between 1 and 2 ppm with the strongest at 1.47 and 1.72 ppm. A sample of **7** was dissolved in cyclohexene and was heated at 70 °C for 24 h. The volatiles were removed *in vacuo*, and the reaction residue was analyzed by <sup>1</sup>H NMR spectroscopy. Resonances due to cyclohexene oligomers appear in the ranges 1–2 and 5.3–5.8 ppm. Key diagnostic peaks due to remaining **7** appear at 1.65, -1.26, and 4.48 ppm. Key diagnostic peaks due to **8** appear at 1.76, 0.54, 5.17, and 7.00 ppm.

**Oligomerization of Cyclohexene and 1,4-Cyclohexadiene with 2 and 3.** The oligomerizations of cyclohexene and 1,4-cyclohexadiene were effected with **2** and **3** in a similar manner. The procedure for cyclohexene with **2** is described as a representative example. A 0.010 M solution was prepared by dissolving **2** (0.027 g, 0.050 mmol) in cyclohexene (5.0 mL). This solution was heated at 100 °C for 24 h, during which time the solution changed color from red to brown. The volatile components were removed from the final mixture *in vacuo* to obtain a viscous brown oil that was redissolved in a minimum of pentane and was transferred to the top of a silica column (ca. 7 × 0.5 cm). The organic products were then eluted from the column with pentane, and solvent removal from the eluate yielded a colorless oil (0.54 g).

Similarly, **3** (0.026 g in 5.0 mL cyclohexene) gave 0.64 g of colorless oil at 100 °C.

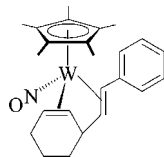
Table 6. X-ray Crystallographic Data for Complexes 7, 8, 9, and 10

	7	8	9	10
	Crystal Data			
empirical formula	C <sub>26</sub> H <sub>41</sub> NO	C <sub>26</sub> H <sub>41</sub> NO	C <sub>24</sub> H <sub>31</sub> NO	C <sub>22</sub> H <sub>31</sub> NO
cryst habit, color	prism, red	prism, yellow	prism, red	needle, pink
cryst size (mm)	0.10 × 0.07 × 0.05	0.45 × 0.40 × 0.35	0.60 × 0.25 × 0.10	0.40 × 0.07 × 0.04
cryst syst	triclinic	monoclinic	orthorhombic	triclinic
space group	<i>P</i> $\bar{1}$	<i>P</i> 2 <sub>1</sub> / <i>a</i>	<i>Pna</i> 2 <sub>1</sub>	<i>P</i> $\bar{1}$
volume (Å <sup>3</sup> )	1154.6(3)	2393.14(14)	2049.84(15)	948.71(14)
<i>a</i> (Å)	9.7773(15)	14.6050(5)	16.8210(7)	8.1917(6)
<i>b</i> (Å)	11.3376(17)	8.6048(3)	12.6397(5)	9.7406(9)
<i>c</i> (Å)	11.7186(18)	20.1135(7)	9.6412(4)	13.6903(13)
$\alpha$ (deg)	77.630(6)	90	90	73.624(3)
$\beta$ (deg)	65.729(5)	108.781(1)	90	89.272(3)
$\gamma$ (deg)	88.019(6)	90	90	65.724(3)
<i>Z</i>	2	4	4	2
density (calcd) (Mg/m <sup>3</sup> )	1.632	1.575	1.728	1.783
absorp coeff (mm <sup>-1</sup> )	5.019	4.843	5.649	6.098
<i>F</i> <sub>000</sub>	572	1144	1056	504
	Data Collection and Refinement			
measd refls: total	17 232	36 804	14 882	26 325
measd refls: unique	5172	9241	3957	4467
final <i>R</i> indices <sup>a</sup>	R1 = 0.0677, wR2 = 0.1773	R1 = 0.0352, wR2 = 0.0864	R1 = 0.0178, wR2 = 0.0386	R1 = 0.0152, wR2 = 0.0335
goodness-of-fit on <i>F</i> <sup>2b</sup>	1.044	1.054	1.035	1.065
largest diff. peak and hole (e <sup>-</sup> Å <sup>-3</sup> )	4.694 and -4.014	2.933 and -1.684	1.571 and -0.735	1.184 and -0.574

<sup>a</sup> R1 on  $F = \sum(|F_o| - |F_c|) / \sum |F_o|$  ( $I > 2\sigma(I)$ ); wR2 =  $[\sum(F_o^2 - F_c^2)^2 / \sum w(F_o^2)]^{1/2}$  (all data);  $w = [\sigma^2 F_o^2]^{-1}$ . <sup>b</sup> GOF =  $[\sum w(|F_o| - |F_c|)^2 / \text{degrees of freedom}]^{1/2}$ .

**<sup>1</sup>H NMR Spectroscopic Monitoring of Transfer Dehydrogenation: Oligomerization of Cyclohexene and 1,4-Cyclohexadiene.** A sample of **2** (10 mg, 0.018 mmol) dissolved in cyclohexene was heated at 60 °C for 24 h in a sealed NMR tube and monitored by <sup>1</sup>H NMR spectroscopy. In addition to resonances due to the substrate and to cyclohexene oligomers, a singlet peak appeared at 1.83 ppm (attributable to cyclohexane). A sample of **2** (10 mg, 0.018 mmol) dissolved in 1,4-cyclohexadiene was heated at 60 °C for 24 h in a sealed NMR tube and monitored by <sup>1</sup>H NMR spectroscopy. In addition to resonances due to the substrate and to 1,4-cyclohexadiene oligomers, a strong singlet peak appeared at 7.16 ppm (attributable to benzene) and a small singlet peak appeared at 1.37 ppm (attributable to cyclohexane).

**Reaction of 2 with Cyclohexene: Preparation of 9.** A resealable reaction vessel was charged with Cp\*W(NO)(CH<sub>2</sub>SiMe<sub>3</sub>)(η<sup>2</sup>-CPhCH<sub>2</sub>) (**2**) (350 mg, 0.65 mmol) and cyclohexene (8 mL). The resulting red solution was then heated at 50 °C for 16 h, and the volatile components were removed from the final reaction mixture under reduced pressure to obtain an oily red solid. This solid was redissolved in a minimum of pentane, and the solution was transferred to the top of a silica column (ca. 6 × 0.5 cm). The organic products were eluted with a large volume of pentane, the remaining red-brown band was eluted with 3:1 pentane/Et<sub>2</sub>O, and the eluate was collected. Removal of the volatile components from the eluate and recrystallization of the residual solid from a mixture of Et<sub>2</sub>O/hexanes at -30 °C afforded complex **9** as bright red crystals (93 mg, 0.17 mmol, 27%).



Anal. Calcd for C<sub>24</sub>H<sub>31</sub>NO: C, 54.05; H, 5.86; N, 2.63. Found: C, 54.14; H, 5.93; N, 2.91. IR (Nujol):  $\nu_{\text{NO}}$  1588 cm<sup>-1</sup>. MS (EI, 120 °C): *m/z* 535 [P<sup>+</sup>]. <sup>1</sup>H NMR (C<sub>6</sub>D<sub>6</sub>, 400 MHz, 25 °C):  $\delta$  -0.97 (1H, t, olefinic-CH), 1.41 (15H, s, C<sub>5</sub>Me<sub>5</sub>), 1.59 (2H, m, (overlapping) cyclohexenyl-CH<sub>2</sub>), 1.83 (1H, dd, (overlapping) olefinic CH), 2.22 (1H, m, olefinic CH), 3.14, 2.65, 1.72, and 1.96 (1H each, m,

(overlapping) cyclohexenyl-CH<sub>2</sub>), 4.61 (1H, m, PhCH=CH), 6.98–6.92 (1H, m, aryl), 7.20–7.18 (3H, m, aryl), cyclohexenyl-allylic proton obscured. <sup>13</sup>C NMR (C<sub>6</sub>D<sub>6</sub>, 400 MHz, 25 °C):  $\delta$  9.3 (C<sub>5</sub>Me<sub>5</sub>), 28.4, 27.7, 17.7 (cyclohexenyl-CH<sub>2</sub>), 30.6 (cyclohexenyl-allylic carbon), 69.2, 48.5, 45.2, 11.2 (olefinic carbons), 102.1 (C<sub>5</sub>Me<sub>5</sub>), 128.6, 126.3, 124.7 (ortho-, meta-, and para-aryl), 146.7 (ipso-aryl).

**<sup>1</sup>H NMR Spectrum of 9 in Cyclohexene after Heating.** A sample of **9** (10 mg, 0.019 mmol) was dissolved in cyclohexene and heated at 50 °C for 16 h. The volatile components were removed *in vacuo*, and the reaction residue was analyzed by <sup>1</sup>H NMR spectroscopy. Resonances due to cyclohexene oligomers appear in the ranges 1–2 and 5.3–5.8 ppm. Key diagnostic peaks due to **9** appear at 1.4 and 4.6 ppm.

**X-ray Crystallography.** Data collection for each compound was carried out at -100 ± 1 °C on a Rigaku AFC7/ADSC CCD diffractometer or on a Bruker X8 APEX diffractometer, using graphite-monochromated Mo K $\alpha$  radiation.

Data for **7** were collected to a maximum  $2\theta$  value of 56.2° in 0.5° oscillations. The structure was solved by direct methods<sup>24</sup> and expanded using Fourier techniques. Disorder at C14 and C15 was modeled as part A (70%) and part B (30%). As a result, C14a, C14b, C15a, and C15b were refined isotropically, and all other non-hydrogen atoms were refined anisotropically. Hydrogen atoms H1, H10, and H11 were refined isotropically, and all other hydrogen atoms were included in fixed positions. The final cycle of full-matrix least-squares analysis was based on 5172 observed reflections and 277 variable parameters.

Data for **8** were collected to a maximum  $2\theta$  value of 66.8° in 0.5° oscillations. The structure was solved by direct methods<sup>24</sup> and expanded using Fourier techniques. The disordered Cp\* ring was modeled in three orientations; the largest contributor was modeled anisotropically and the two lesser contributors were modeled isotropically. All other non-hydrogen atoms were refined anisotropically. Hydrogen atoms H1, H10, and H11 were refined isotropically, and all other hydrogen atoms were included in fixed positions. The hydride on the tungsten center could not be modeled.

(24) SIR92. Altomare, A.; Cascarano, M.; Giacovazzo, C.; Guagliardi, A. *J. Appl. Crystallogr.* **1993**, *26*, 343.

The final cycle of full-matrix least-squares analysis was based on 9241 observed reflections and 271 variable parameters.

Data for **9** were collected to a maximum  $2\theta$  value of  $55.8^\circ$  in  $0.5^\circ$  oscillations. The structure was solved by direct methods<sup>24</sup> and expanded using Fourier techniques. All non-hydrogen atoms were refined anisotropically; hydrogen atoms H1, H2, H7, and H8 were refined isotropically, and all other hydrogen atoms were included in fixed positions. The final cycle of full-matrix least-squares analysis was based on 3957 observed reflections and 265 variable parameters.

Data for **10** were collected to a maximum  $2\theta$  value of  $55.8^\circ$  in  $0.5^\circ$  oscillations. The structure was solved by direct methods<sup>24</sup> and expanded using Fourier techniques. All non-hydrogen atoms were refined anisotropically; hydrogen atoms H2, H3, H8, H9, and H10 were refined isotropically, and all other hydrogen atoms were included in fixed positions. The final cycle of full-matrix least-squares analysis was based on 4467 observed reflections and 251 variable parameters.

For each structure neutral-atom scattering factors were taken from Cromer and Waber.<sup>25</sup> Anomalous dispersion effects were included in  $F_{\text{calc}}$ ;<sup>26</sup> the values for  $\Delta f'$  and  $\Delta f''$  were those of Creagh and McAuley.<sup>27</sup> The values for mass attenuation coefficients are those

of Creagh and Hubbell.<sup>28</sup> All calculations were performed using the CrystalClear software package of Rigaku/MSC,<sup>29</sup> or Shelxl-97.<sup>30</sup> X-ray crystallographic data for the four structures are presented in Table 6 and in the cif files provided as Supporting Information.

**Acknowledgment.** We are grateful to the Natural Sciences and Engineering Research Council of Canada for support of this work in the form of grants to P.L. and a postgraduate scholarship to M.S.A.B. We also thank Dr. E. Tran and Mr. X. Jin for their preliminary contributions to this work.

**Supporting Information Available:** CIF files providing full details of crystallographic analyses of complexes **7**, **8**, **9**, and **10**. Also representative EIMS, GC/MS, and NMR spectra for the cyclohexene oligomers and dimers and for the 1,4-cyclohexadiene oligomers, and sample spectra for the *in situ* NMR experiments. This material is available free of charge via the Internet at <http://pubs.acs.org>.

OM800384Z

---

(25) Cromer, D. T.; Waber, J. T. *International Tables for X-ray Crystallography*; Kynoch Press: Birmingham, 1974; Vol. IV.

(26) Ibers, J. A.; Hamilton, W. C. *Acta Crystallogr.* **1964**, *17*, 781–782.

(27) Creagh, D. C.; McAuley, W. J. *International Tables of X-ray Crystallography*; Kluwer Academic Publishers: Boston, 1992; Vol. C.

---

(28) Creagh, D. C.; Hubbell, J. H. *International Tables for X-ray Crystallography*; Kluwer Academic Publishers: Boston, 1992; Vol. C.

(29) *CrystalClear*, Version 1.3.5b20; Molecular Structure Corporation, 2002.

(30) Sheldrick, G. M. *SHELXL97*; University of Göttingen: Germany, 1997.